Journal of Bioenergetics and Biomembranes, Vol. 26, No. 1, 1994

Structure–Function Studies of [2Fe-2S] Ferredoxins

Hazel M. Holden,[1,4] Bruce L. Jacobson,[1] John K. Hurley,[2] Gordon Tollin,[2] Byung-Ha Oh,[3,5] Lars Skjeldal,[3,6] Young Kee Chae,[3,4] Hong Cheng,[3] Bin Xia,[3,4] and John L. Markley[3,4]

Received September 12, 1993; accepted October 5, 1993

The ability to overexpress [2Fe-2S] ferredoxins in *Escherichia coli* has opened up exciting research opportunities. High-resolution x-ray structures have been determined for the wild-type ferredoxins produced by the vegetative and heterocyst forms of *Anabaena* strain 7120 (in their oxidized states), and these have been compared to structural information derived from multidimensional, multinuclear NMR spectroscopy. The electron delocalization in these proteins in their oxidized and reduced states has been studied by ^{1}H, ^{2}H, ^{13}C, and ^{15}N NMR spectroscopy. Site-directed mutagenesis has been used to prepare variants of these ferredoxins. Mutants (over 50) of the vegetative ferredoxin have been designed to explore questions about cluster assembly and stabilization and to determine which residues are important for recognition and electron transfer to the redox partner *Anabaena* ferredoxin reductase. The results have shown that serine can replace cysteine at each of the four cluster attachment sites and still support cluster assembly. Electron transfer has been demonstrated with three of the four mutants. Although these mutants are less stable than the wild-type ferredoxin, it has been possible to determine the x-ray structure of one (C49S) and to characterize all four by EPR and NMR. Mutagenesis has identified residues 65 and 94 of the vegetative ferredoxin as crucial to interaction with the reductase. Three-dimensional models have been obtained by x-ray diffraction analysis for several additional mutants: T48S, A50V, E94K (four orders of magnitude less active than wild type in functional assays), and A43S/A45S/T48S/A50N (quadruple mutant).

KEY WORDS: [2Fe-2S] ferredoxins; electron transport; x-ray crystallography; nuclear magnetic resonance spectroscopy; fast reaction kinetics; mutagenesis; iron-sulfur cluster assembly; heterologous expression; stable-isotope labeling; *Anabaena*.

1. INTRODUCTION

Two-iron two-sulfur, [2Fe-2S], clusters constitute a structural–functional motif that is widely used in proteins. In the [2Fe-2S] ferredoxins, this cluster serves as a site of one-electron oxidation or reduction. The literature contains a wealth of protein sequences for ferredoxins, particularly photosynthetic (plant-type) [2Fe-2S] ferredoxins (Matsubara *et al.*, 1980; Matsubara and Hase, 1983), and a recent homology search has been compiled for this protein class (Barker *et al.*, 1992). Figure 1 compares the sequences of five [2Fe-2S] ferredoxins that have been studied extensively. *Spirulina platensis* ferredoxin and *Anabaena* 7120 vegetative ferredoxin are "plant-type" ferredoxins (from cyanobacteria), which serve as an electron carrier from photosystem I to ferredoxin-$NADP^{+}$ reductase (FNR). FNR, in turn, catalyzes

[1] Institute for Enzyme Research, University of Wisconsin-Madison, Madison, Wisconsin 53705-4098.
[2] Department of Biochemistry, University of Arizona, Tucson, Arizona 85721-0002.
[3] Department of Biochemistry, University of Wisconsin-Madison, Madison, Wisconsin 53706-1569.
[4] Graduate Program in Biophysics, University of Wisconsin-Madison, Madison, Wisconsin 53706-1569.
[5] Present address: SmithKline Beecham, 709 Swedeland Road, P.O. Box 1539, King of Prussia, Pennsylvania 19406-0939.
[6] Present address: Department of Biochemical Sciences, Agricultural University of Norway, IBF, Kjemi boks 5040, N-1432 ÅS, Norway.

0145-479X/94/0200-0067$07.00/0

```
Spirulina platensis          ATYKVTLINE-AEGINETIDCDDDTYILDAA--EEAGLDLPYSCRA-GACSTCAGTITS
Anabaena 7120 vegetative     ATFKVTLINE-AEGTKHEIEVPDDEYILDAA--EEQGYDLPFSCRA-GACSTCAGKLVS
Anabaena 7120 heterocyst     ASYQVRLINK-KQDIDTTIEIDEETTILDGA--EENGIELPFSCHS-GSCSSCVGKVVE
Human mitochondrial        SSSEDKITVHIFINRDGETLTTKGKVGDSLLDVVVENNLDIDGFGACEGTLACSTCHLIFED
Bovine adrenal             SSSEDKITVHIFINRDGETLTTKGKIGDSLLDVVVQNNLDIDGFGACEGTLACSTCHLIFEQ
Putidaredoxin                    SKVVYVSHDG-TRRELDVADGVSLMQAAVSNGIYDIVGDCGGSASCATCHVYVNE

Spirulina platensis          GTIDQSD------QSFLD--DDQIEAGYVLTCVAYPTSDCTIKTHQEEGLY
Anabaena 7120 vegetative     GTVDQSD------QSFLD--DDQIEAGYVLTCVAYPTSDVVIQTHKEEDLY
Anabaena 7120 heterocyst     GEVDQSD------QIFLD--DEQMGKGFALLCVTYPRSNCTIKTHQEPYLA
Human mitochondrial          HIYEKLDAITDEENDMLD-LAYGLTDRSRLGCQICLTKSMDNMTVRVPETVADARQSIDVGKTS
Bovine adrenal               HIFEKLEAITDEENDMLD-LAYGLTDRSRLGCQICLTKAMDNMTVRVPDAVSDARESIDMGMNSSKIE
Putidaredoxin                AFTDKVPAANEREIGMLECVTAELKPNSRLCCQIIMTPELDGIVVDVPDRQW
```

Fig. 1. Comparison of the sequences of representative ferredoxins. (1) Plant-type: *Spirulina platensis* (Tanaka *et al.*, 1976), *Anabaena* 7120 vegetative (Alam *et al.*, 1986), *Anabaena* 7120 heterocyst (Böhme and Haselkorn, 1988); (2) vertebrate-type: human mitochondrial (Mittal *et al.*, 1988), bovine adrenal (Okamura *et al.*, 1985; Cupp and Vickery, 1988); (3) bacterial-type: putidaredoxin (Peterson *et al.*, 1990). Cysteine ligands to the iron-sulfur cluster are underlined.

the reduction of $NADP^+$ to NADPH (Masaki *et al.*, 1982). *Anabaena* 7120 heterocyst ferredoxin, also a "plant-type" ferredoxin, is found only in cyanobacterial cells that have differentiated into nitrogen-fixing cells (heterocysts). Heterocyst ferredoxin, which also is capable of functioning in photosynthetic electron transport, plays a role in nitrogen fixation by transferring an electron to the iron-protein of nitrogenase (Böhme and Schrautemeier, 1987); the vegetative ferredoxin, however, has a more limited specificity, and cannot function in the nitrogen fixation electron transport pathway. Human placental and bovine adrenal (adrenodoxin) ferredoxins are representative "vertebrate-type" ferredoxins, which serve to transfer electrons from NADPH-dependent ferredoxin reductase to the cytochrome P450 enzymes involved in the biogenesis of steroid hormones, the formation of vitamin D metabolites, and the production of bile acids (Mason and Boyd, 1971). The ferredoxin from *Pseudomonas putida* (putidaredoxin) is a "bacterial-type" ferredoxin whose sequence (Peterson *et al.*, 1990) shows strong resemblance to the vertebrate ferredoxins. It acts as a specific reductant to cytochrome $P\text{-}450_{cam}$ isolated from the same organism (Cushman *et al.*, 1967). The ferredoxin isolated from *Escherichia coli* (Ta and Vickery, 1992) also appears to belong to this class.

Until recently, the Protein Data Bank (Bernstein *et al.*, 1977) contained only one ferredoxin structure, that of the plant-type ferredoxin from *Spirulina platensis* (Tsukihara *et al.*, 1981). The new x-ray structures of the photosynthetic (Rypniewski *et al.*, 1991) and nitrogen-fixing (Jacobson *et al.*, 1992) ferredoxins from *Anabaena* 7120 have expanded the base of structural information, but complete structures are lacking still for representative vertebrate- and bacterial-type [2Fe-2S] ferredoxins.

The first NMR study of a [2Fe-2S] ferredoxin was the report of hyperfine signals by Poe *et al.* (1971). Dunham *et al.* (1971) presented a theoretical analysis of hyperfine shifts of [2Fe-2S] ferredoxins later the same year. The inherent paramagnetism of [2Fe-2S] ferredoxins complicates the NMR assignment problem. One approach to assigning diamagnetic signals has been to compare the spectra of mutant proteins; this approach has led to assignments in plant-type (Chan *et al.*, 1983a) and vertebrate-type ferredoxins (Miura and Ichikawa, 1991). A second approach has been to label ferredoxins uniformly with carbon-13 to facilitate spectral analysis (Chan and Markley, 1982). With *Anabaena variabilis* ferredoxin labeled uniformly with ^{13}C, it was possible to study the interaction of ferredoxin with spinach ferredoxin reductase and to identify the region of the ferredoxin that contacts the reductase (Chan *et al.*, 1983b). The introduction of multinuclear, multidimensional NMR methods (Stockman and Markley, 1990) have led to more robust, concerted assignment methods. The application of modern, isotope-assisted methods to ferredoxins has been facilitated by the development of methods for heterologous overexpression of [2Fe-2S] ferredoxins in *E. coli* and for reconstitution of the iron-sulfur cluster *in vitro* (Coghlan and Vickery, 1989).

Greenfield *et al.* (1989) carried out the first NMR studies on a vertebrate-type ferredoxin (adrenodoxin) but examined only the diamagnetic part of that spectrum. Miura and Ichikawa (1991a,b) assigned a number of aromatic resonances in bovine adrenodoxin by comparing spectra of different mitochondrial ferre-

doxins, and they have interpreted chemical shift changes that occur upon reduction in terms of a conformational change. Pochapsky and coworkers (Pochapsky and Ye, 1991; Ye *et al.*, 1992) have obtained backbone assignments for putidaredoxin and have assembled these into a β-sheet structure that resembles that found in the other [2Fe-2S] ferredoxins whose structures are known.

Iron-sulfur proteins have recently become subjects for site-directed mutagenesis studies. Coghlan and Vickery (1991) used mutation studies to identify residues that are critical to the binding of human ferredoxin to cytochrome P-450*scc*. Rothery and Weiner (1991) have mutated one of the cysteine ligands in a [4Fe-4S] cluster in *E. coli* dimethyl sulfoxide reductase (Cys^{102}) to Trp, Ser, Tyr, and Phe. All four mutants had altered EPR properties in the oxidized and reduced states which indicated that the cluster had been converted to [3Fe-4S]; the mutants also had altered redox activity. Werth *et al.* (1990) have mutated to serine all four N-terminal cysteine residues in the FrdB subunit of *E. coli* fumarate reductase which participate in a [2Fe-2S] cluster. The mutations lowered the reduction potential of this center and reduced enzymatic activity. The Sligar group (Gerber *et al.*, 1990) has mutated cysteine residues 73, 85, and 86 of putidaredoxin to serines and found that only C85S and C73S express holoprotein as evidenced by SDS-PAGE and EPR spectroscopy; they concluded as a result that residues 39, 45, 48, and 86 are the iron-sulfur ligands. Site-directed mutagenesis offers the means of testing the factors believed to be important in determining the redox potential of ferredoxin: (1) the extent and localization of hydrogen bonds to the cluster (Tsukihara *et al.*, 1986), (2) the nature of the coordinating ligands (Gurbiel *et al.*, 1989), and (3) the polarity of the cluster environment (Tsukihara *et al.*, 1986; Kassner and Yang, 1977).

Important progress has been made recently in structural studies of the protein to which photosynthetic ferredoxins pass an electron. Zanetti *et al.* (1987, 1988) have carried out chemical modification and cross-linking experiments that have identified regions of the ferredoxin that are important for its interaction with FNR. Karplus *et al.* (1991) have determined an x-ray structure for spinach FNR at 2.2 Å resolution.

This article summarizes recent results from the authors' laboratories that address structure–function issues of [2Fe-2S] ferredoxins. These results are discussed in the context of work carried out in other laboratories.

2. PROTEIN PREPARATION AND CHARACTERIZATION

2.1. Source of Ferredoxin Genes

The gene for *Anabaena* 7120 vegetative ferredoxin (Alam *et al.*, 1986) was a gift from Dr. Stephanie Curtis; wild-type and mutated versions of this protein have been produced independently in the Markley and Tollin laboratories. The gene for *Anabaena* 7120 heterocyst ferredoxin (Böhme and Haselkorn, 1988, 1989), was provided by Dr. Herbert Böhme; the recombinant protein (wild-type and mutants) has been produced in the Markley laboratory. The gene for human placental ferredoxin (Mittal *et al.*, 1988) was supplied by Dr. Larry Vickery who is collaborating with the Markley group on NMR studies of wild-type and mutant versions of this ferredoxin.

2.2. Overproduction and Reconstitution of Ferredoxins

Full details are provided elsewhere for procedures used at the University of Wisconsin-Madison for subcloning, mutagenesis, overexpression, and reconstitution of the *Anabaena* 7120 heterocyst (Chae *et al.*, 1993) and vegetative (Cheng *et al.*, 1993a) ferredoxins and the human ferredoxin (Xia *et al.*, 1993).

For the *Anabaena* 7120 heterocyst ferredoxin construct, the cloned structural gene (*fdx* H; Böhme and Haselkorn, 1988) in a *pUC* plasmid (Böhme and Haselkorn, 1989) was subcloned into the overexpression vector *pET-9a*(-) [a slightly modified form of the original *pET-9a* vector (Novagen, Madison, Wisconsin) in which one of the restriction sites had been deleted] behind the T7 promoter by making use of two restriction sites (*NheI* and *BamHI*). The resulting plasmid, in which the heterocyst ferredoxin gene is under control of the T7 promoter, is named *pKID*. This plasmid was transformed into *E. coli* strain BL-21(DE3), which has the T7 RNA polymerase gene in its chromosome along with another plasmid, *pLysS*, which serves to suppress the basal level expression of the heterocyst ferredoxin before induction. Protein production and reconstitution have been described

(Jacobson *et al.*, 1992). Typical yields of reconstituted heterocyst ferredoxin are around 20 mg/liter culture.

Construction of the T7 overexpression system for the *Anabaena* 7120 vegetative ferredoxin was more complicated because the original DNA fragment *pAn662* (obtained from S. Curtis), which contains the structural gene *petF*, did not contain suitable restriction enzyme sites. The entire gene coding region for the vegetative ferredoxin, *petF*, was first amplified *in vitro* by the polymerase chain reaction, and two new restriction enzyme sites, *Nde I* at 5′ and *BamHI* at 3′, were introduced by oligonucleotide-directed mutagenesis. The amplified DNA fragment was purified, and a blunt-ended DNA fragment was inserted into the *SmaI* site of *pIBI* 25 vector DNA (IBI, New Haven, Connecticut). The ligated DNA was transformed into TG1-competent *E. coli* cells and spread on LB plates containing 50 μg/mL of ampicillin, 5μL of isopropylthiogalactoside (IPTG) (200 mg/mL), and 40 μL of X-gal (20 mg/mL). Cells containing inserted ferredoxin DNA fragments were picked by blue/white selection. The plasmid DNA was purified by standard procedures and verified by digestion with restriction enzymes, *Nde I* and *BamH I*. The sequence of the polymerase chain reaction amplified DNA fragment has been verified by DNA sequencing. Then a DNA fragment, which contained the entire ferredoxin gene coding region, *petF*, was released by digestion with two restriction enzymes, *Nde I* and *BamH I*. The digested DNA fragment was purified from a low-melting-temperature agarose gel and then ligated into *Nde I* and *BamH I* cleaved *pET9a*. The ligated DNA was transformed into *E. coli* HMS174 competent cells. After checking by digestion, the plasmid DNA containing the inserted ferredoxin gene *petF* gene was transformed into *BL21/pLysS E. coli* competent cells. Typically, a single colony (e.g., *BL21/pET9a/F*) was grown at 37°C overnight in 5-mL LB medium supplemented with kanamycin (100 μg/mL) and chloramphenicol (34 μg/mL). This culture was used to inoculate a 1-L LB-kanamycin-chloramphenicol culture. When $OD_{550} = 1.2$ was reached, 100 mg IPTG (isopropylthiogalactoside) was added to induce ferredoxin production. After an additional 2-h incubation at 37°C, the cells were harvested by centrifugation. The cellular pellets were resuspended in 20 mL of 50 mM potassium phosphate buffer at pH 7.4 and then lysed by a freeze–thawing cycle. After addition of 0.1% triton X-100 to the cell lysate, the suspension was sonicated. Ultrapure urea was added to the solution to achieve 6 M concentration. The ferredoxin was then reconstituted by following the procedure of Coghlan and Vickery (1989). Briefly, the reaction mixture was degassed under vacuum, and dithiothreitol (DTT) was added to a final concentration of 100 mM. Under bubbling argon gas, $FeCl_3$, $Fe(NH_4)_2(SO_4)_2$, and Na_2S were then added gradually to a final concentration of 1 mM each. The mixture is incubated for an additional 10 min with stirring and flushing with an argon gas, then immediately diluted eightfold with degassed 50 mM potassium phosphate buffer, pH of 7.4. The reconstituted ferredoxin was further purified by ion-exchange chromatography followed by gel filtration. Typical yields of the reconstituted vegetative ferredoxin were about 20 mg/L culture.

At the University of Arizona, the structural gene for the vegetative ferredoxin, *petF*, from *Anabaena* sp. strain PCC 7120 (Alam *et al.*, 1986), was incorporated as a *HindIII* fragment into the expression vector *pIBI25* (IBI, New Haven, Connecticut), and the resulting plasmid (*pAn662*) (obtained from Dr. Stephanie Curtis) was used directly for protein expression and site-directed mutagenesis studies. The procedure used at the University of Arizona for production of *Anabaena* 7120 vegetative ferredoxin employed *E. coli* strain *JM109*, which had been transformed with the plasmid *pAn662*. From a 1-L inoculum, a 16-L culture was grown overnight (16–17 h) at 37°C with shaking in LB media containing 150 μg ampicillin/ml and 60 μM $FeSO_4$ (Böhme and Haselkorn, 1989). Cells were harvested by centrifugation and lysed by a modification of a standard procedure (Sambrook *et al.*, 1989) which employs lysozyme treatment followed by treatment with DNAse I (Calbiochem, San Diego, California, from bovine pancreas). Following sonication and high-speed centrifugation, ferredoxin was purified from the supernatant by chromatography on DEAE-cellulose and Sephadex G50-f (Pharmacia, Uppsala, Sweden). Fractions having an A_{422}/A_{276} ratio greater than 0.5 were pooled for use in kinetic and spectroscopic experiments. For some ferredoxins, an additional step of ammonium sulfate fractionation was necessary to achieve the purity ratio given above. Yields of pure protein ranged between 3 and 12 μmol.

2.3. Site-Directed Mutagenesis

Mutants of *Anabaena* vegetative and heterocyst ferredoxin prepared at the University of Wisconsin-

Madison employed the Kunkel *et al.* (1987) method. Oligonucleotides for mutagenesis and sequencing were synthesized on a 0.2 mmol scale in the DNA synthesis facility in the Department of Biochemistry and were purified by using QIAGEN-tip columns (QIAGEN, Chatsworth, California). Mutagenesis was performed by using single-stranded M13 (*mp18/pet9a/F*) DNA as a template. *E. coli* strain JM103 was used for the mutagenesis. The mutants were identified by DNA sequencing according to the Sequenase protocol (United States Biochemical Corp.) by using the standard dideoxynucleotide chain termination method (Sanger *et al.*, 1977). After mutagenesis, the mutated *EcoR I-Sal I* DNA fragment containing the *pet F* region was cloned back into *pET9a* to restore the complete expression vector. The plasmid DNA purified from *E. coli* strain HMS174 was transformed into the expression host cell, BL21(DE3)/*pLysS*.

Site-directed mutants of *Anabaena* vegetative ferredoxin made at the University of Arizona used the unique site elimination (USE) method of Deng and Nickoloff (1992) which is available in kit form (Transformer Mutagenesis Kit, Clontech, Palo Alto, California). Oligonucleotide primers for mutagenesis ranged from 20 to 32 bases in length. Base changes within the mutagenic oligonucleotides were made such that the resulting codons were those most frequently used by *E. coli* (Springer and Sligar, 1987). Molecular biology procedures (restriction digestion, ligation, transformation, DNA sequencing, etc.) followed standard procedures (Sambrook *et al.*, 1989; Ausubel *et al.*, 1989). DNA from transformed bacteria (*E. coli*, strain JM109) was isolated and purified (Magic Minipreps DNA Purification System, Promega, Madison, Wisconsin) and colonies containing the appropriate mutant proteins were identified by double-stranded DNA sequence analysis.

2.4. Stable Isotope Labeling of the Protein for NMR Studies

Protein samples were prepared by using the T7 expression system. Uniform labeling for NMR spectroscopy was achieved by growing the *E. coli* host cells on minimal media containing [99% ^{15}N]ammonia (for single complete labeling) or [99% ^{15}N]ammonia plus [99% UL ^{13}C]glucose (for double complete labeling). Suitable auxotrophic strains were developed for the introduction of individual ^{15}N or ^{13}C labeled amino acids (selective labeling).

Table I. Rate Constants[a] for Reduction of Wild-Type and Mutant *Anabaena* Ferredoxins by dRfH$^{\bullet}$ and Their Oxidation by *Anabaena* FNR, and Selected Ferredoxin Reduction Potentials and FNR Dissociation Constants

	$k \times 10^{-8}$, $M^{-1} s^{-1}$			
	dRfH$^{\bullet}$	FNR	$E_{1/2}$[b] (mV)	K_d[c] (μM)
wt[d]	2.2 ± 0.2	1.2 ± 0.1	-440 ± 15	9 ± 1
D68K/D69K	1.4 ± 0.2	1.1 ± 0.1	nd	nd
D68K	1.3 ± 0.2	1.9 ± 0.2	nd	nd
E94K/E95K	2.5 ± 0.4	~ 0.00007	nd	nd
E95K	1.7 ± 0.1	1.2 ± 0.1	nd	nd
E94K	2.6 ± 0.4	~ 0.00005	-435 ± 15	26 ± 3
R42A	1.4 ± 0.2	2.0 ± 0.3	nd	nd
R42H	1.3 ± 0.2	2.0 ± 0.2	nd	nd
T48A	1.3 ± 0.3	1.6 ± 0.2	nd	nd
F65A	1.2 ± 0.2	~ 0.00007	-445 ± 15	120 ± 10
F65I	1.1 ± 0.1	~ 0.0002	nd	nd
F65W	1.2 ± 0.2	0.9 ± 0.1	nd	nd
F65Y	1.5 ± 0.2	1.3 ± 0.2	nd	nd
S64Y/F65A	1.6 ± 0.1	~ 0.00005	nd	nd
HFd	1.3 ± 0.1	1.8 ± 0.2	-445 ± 0.2	nd

[a] Rate constants were measured at an ionic strength of 12 mM; data from Hurley *et al.* (1993a), except for F65W, F65Y, and S64Y/F65A which are from Hurley *et al.* (1993b).

[b] The $E_{1/2}$ value is versus NHE (see Hurley *et al.*, 1993a, for details).

[c] K_d values were measured at $I = 12$ mM and were calculated as described by Hurley *et al.* (1993a).

[d] Abbreviations: wt, wild type; Hfd heterocyst ferredoxins; all mutants are in the vegetative ferredoxin (VFd) background as indicated by the one-letter amino acid abbreviations (aa) and residue numbers (#): $aa_{VFd}\#aa_{mutant}$.

2.5. Characterization by UV/VIS, CD, NMR and Redox Potential Measurements

The UV/VIS, optical, and CD absorption spectra of the mutant ferredoxins listed in Table I were essentially indistinguishable from those of wild-type ferredoxin (Hurley *et al.*, 1993a), indicating that no appreciable changes in Fe/S cluster environment or protein folding had occurred as a consequence of these mutations.

The reduction potential of recombinant wild-type ferredoxin (wt Fd) is -440 mV (vs. NHE), as measured by cyclic voltammetry (Salamon and Tollin, 1992) utilizing a gold electrode modified with a lipid bilayer consisting of a 1:1 mixture of egg phosphatidylcholine and dioctadecyldimethylammonium chloride. Reduction potentials determined for mutants F65A and E94K, which showed dramatically reduced reactivity with FNR (see below), were found to be unaltered from those of the wild-type (Hurley *et al.*, 1993a).

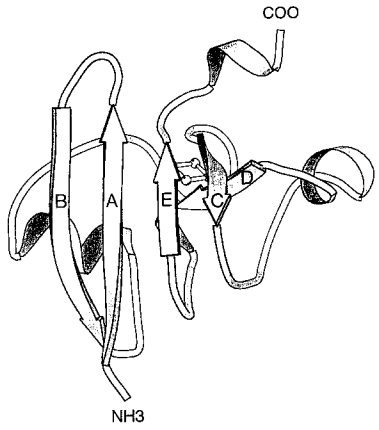

Fig. 2. Ribbon representation of the *Anabaena* ferredoxin, vegetative form. This image was generated by the software MOLSCRIPT (Kraulis, 1991). The five strands of β-pleated sheet are labeled A–E.

3. X-RAY STUDIES OF *ANABAENA* FERREDOXINS

3.1. X-ray Models of the *Anabaena* 7120 Vegetative and Heterocyst Ferredoxins

The molecular structure of the oxidized form of the *Anabaena* [2Fe-2S] vegetative ferredoxin was solved by x-ray crystallographic analysis at 2.5 Å resolution and has since been refined to 1.7 Å resolution with a crystallographic *R*-factor of 17.9% (Rypniewski *et al.*, 1991; Jacobson *et al.*, 1993a). The electron density for the refined model is in complete agreement with the published gene sequence (Alam *et al.*, 1986).

Of the 98 amino acid residues constituting the polypeptide chain, 74% adopt dihedral angles typical for α-helices, β-pleated sheets, and reverse turns. As can be seen in Figs. 2 and 3, the molecular architecture of the molecule is dominated by a mixed β-pleated sheet motif. Specifically, this secondary structural element contains five β-strands, labeled A–E and composed of residues Thr 2 to Asn 9, Thr 14 to Val 20, Ala 50 to Asp 59, Tyr 75 to Leu 77, and Tyr 82 to Thr 91. The topology of the mixed β-sheet is such that strands A, D, and E are parallel to one another and antiparallel to strands B and C. The hydrogen bonding patterns of β-strands C and E are interrupted by the presence of β-bulges, and β-strand D is rather short with only three amino acid residues.

Other secondary structural elements found in the vegetative ferredoxin include six Type I turns (Glu 10 to Gly 13, Asp 22 to Tyr 25, Glu 31 to Gly 34, Ser 47 to Ala 50, Gln 60 to Gln 63, and Ile 71 to Gly 74), two α-helices (Ile 26 to Glu 32 and Asp 68 to Glu 72), and an α-helical turn at the C-terminus delineated by residues Glu 94 to Leu 97. The [2Fe-2S] cluster is located toward one end of the molecule and is ligated to the protein via cysteinyl residues 41, 46, 49, and 79. Only Cys 49 is positioned in a standard secondary structural element.

In the three-dimensional models of plant-type ferredoxins determined thus far from the cyanobacteria, *Spirulina platensis*, *Aphanothece sacrum*, and *Anabaena* 7120, and from *Halobacterium marismortui* of the Dead Sea, the iron-sulfur complex is bound near the protein surface in a structurally conserved loop which extends as much as 9 Å away from the main body of the molecule and adopts ϕ, ψ angles not typical of standard secondary structural elements (Fukuyama *et al.*, 1980, Tsukihara *et al.*, 1990; Rypniewski *et al.*, 1991; Sussman *et al.*, 1989). This surface loop, which comprises 13 amino acid residues, in the *Anabaena* ferredoxin begins at Pro 38 and ends at Ala 50, as shown in stereo in Fig. 4. Excluding Phe 39 and Arg 42, the residues located in this loop in the *Anabaena* molecule have rather small side chains.

The four covalent bonds from the protein cysteinyl residues to the irons of the metal center presumably play significant roles in maintaining the overall three-dimensional integrity of the protein and of this rather precarious surface loop. In addition, this region of the polypeptide chain is further stabilized by a salt

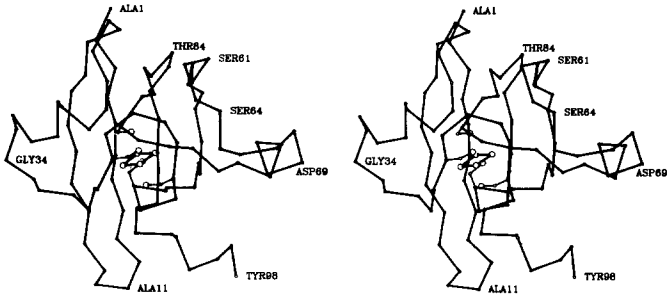

Fig. 3. Stereo view if the *Anabaena* ferredoxin α-carbon backbone, vegetative form. This image was prepared with the plotting software package PLUTO, originally written by Dr. Sam Motherwell and modified for proteins by Eleanor Dodson and Phil Evans. The cysteinyl residue side chains (41, 46, 49, and 79) ligating the cluster to the protein are depicted as ball-and-stick models.

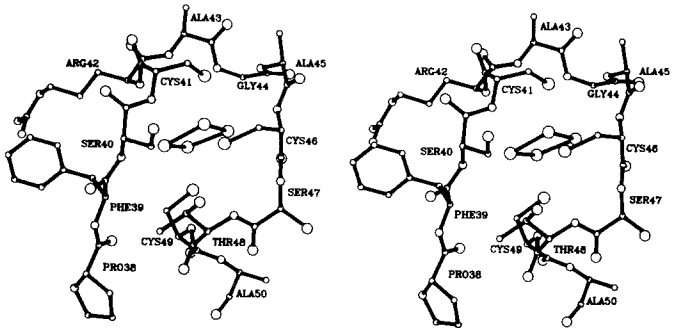

Fig. 4. Stereo view of the metal cluster binding loop. The backbone dihedral angles for the amino acid residues constituting the binding loop do not fall into the classical category of reverse turns.

bridge and by strong hydrogen bonding interactions between evolutionarily conserved amino acid residues. The salt bridge involves Arg 42, which is strictly conserved in 22 of the 26 plant-type [2Fe-2S] ferredoxins reviewed by Matsubara and Hase (1983). Furthermore, this residue was recognized as critical for the proper folding and function of the *S. platensis* ferredoxin (Tsukihara *et al.*, 1981). In the x-ray model for the *Anabaena* vegetative ferredoxin, the role of Arg 42 in stabilizing the [2Fe-2S] binding region is clearly defined; it forms a salt bridge with Glu 31, which is located in a Type I turn. Specifically, $N^{\eta 1}$ and $N^{\eta 2}$ of Arg 42 are 2.8 and 2.7 Å, respectively, from $O^{\epsilon 2}$ and $O^{\epsilon 1}$ of Glu 31. Not surprisingly, Glu 31 is also strictly conserved, except for two cases, in the ferredoxin sequence alignments of Matsubara and Hase (1983). Interestingly, Arg 42 is not conserved in the heterocyst form of the *Anabaena* ferredoxin discussed below.

A schematic diagram of the evolutionarily conserved hydrogen bonding pattern exhibited by the [2Fe-2S] binding loop is given in Fig. 5. This network of electrostatic interactions, involving Ser 47 O^{γ}, Glu 94 N, Glu 94 $O^{\epsilon 1}$, Glu 94 $O^{\epsilon 2}$, Thr 48 O^{γ}, Thr 48 O, Val 50 O, and two solvent molecules, stabilizes the [2Fe-2S] complex binding loop by tethering it to the short C-terminal α-helix. Additionally, both the backbone amide nitrogen and the side chain of Ser 64 are within hydrogen-bonding distance of the carbonyl oxygen of Glu 44. This serine residue is also highly conserved among the plant-type ferredoxin amino acid sequences (Matsubara and Hase, 1983). Collectively, the Glu 31 : Arg 42 salt bridge, the Ser 47, Thr 48, Val 50, Glu 94 hydrogen bonding network, and the electrostatic interactions of Ser 64 serve to anchor the [2Fe-2S] metal center binding loop to three distinct regions of the protein. This tripod-like geometry, along with the thiolate ligands to the irons, undoubtedly stabilizes an area of protein structure that would otherwise be highly flexible.

One novel feature of the *Anabaena* x-ray structure is the ring of solvent molecules surrounding Phe 39, the second amino acid residue in the evolutionarily conserved metal center binding loop. Five well-ordered water molecules are located within 3.4 to 3.8 Å of its aromatic side chain. These solvent molecules are hydrogen bonded to each other with average oxygen-to-oxygen distances of 3.0 Å. The electron density for this region is displayed in stereo in Fig. 6. The local secondary structure of the cluster loop forces Phe 39 into a solvent-exposed position. One potential role for

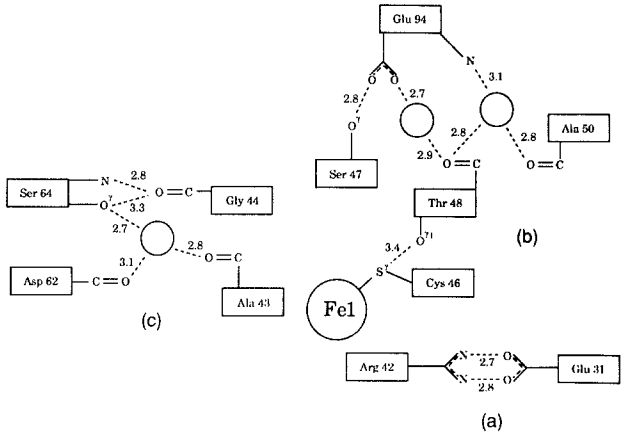

Fig. 5. Schematic representation of the three conserved electrostatic interactions that stabilize the [2Fe-2S] binding loop in the *Anabaena* vegetative ferredoxin.. The large circles represent ordered water molecules. All distances are measured in Ångströms. (a) Salt-bridge between Glu 31 and Arg 42; (b) hydrogen bonding network between Ser 47, Thr 48, Val 50, and Glu 94; (c) electrostatic interactions involving Ser 64.

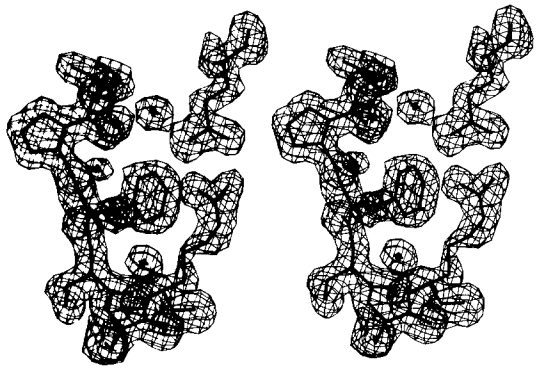

Fig. 6. Portion of the electron density map calculated to 1.7 Å resolution for the vegetative *Anabaena* ferredoxin. The electron density shown was contoured at 1σ and calculated with coefficients of the form $(2F_o - F_c)$, where F_o was the observed structure factor amplitude and F_c was the calculated structure factor amplitude. As can be seen, Phe 39 is surrounded by five ordered water molecules on one side and a salt bridge formed by Arg 42 and Glu 31 on the other.

such a conserved, solvent-exposed aromatic amino acid may be in redox partner recognition.

A close-up view of those amino acid residues located within approximately 3.5 Å of the [2Fe-2S] cluster for the *Anabaena* model is given in Fig. 7. The irons and inorganic sulfurs of the prosthetic group adopt a planar conformation with average iron-sulfur bond lengths of 2.2 Å. The irons are tetrahedrally coordinated with average sulfur-iron-sulfur bond angles of 107°. As indicated by the dashed lines in Fig. 7, five potential hydrogen bonds link backbone amide hydrogens to the γ-sulfurs of the cysteinyl ligands, and three hydrogen bonds link amide hydrogens to inorganic sulfurs of the cluster. No water molecules are located closer than approximately 6.0 Å to the [2Fe-2S] cluster.

It was once thought that the extent of hydrogen bonding to metal clusters plays a crucial role in the modulation of the redox potentials for iron-sulfur proteins. It has become apparent within the last several years, however, that the role of such electrostatic interactions in redox potential modulation may not be as important as once presumed (Backes *et al.*, 1991). For example, the recent three-dimensional structural determinations of the high-potential iron-sulfur proteins isolated from *Ectothiorhodospira halophila* and *Rhodocyclus tenuis* have demonstrated that the vastly differing oxidation–reduction potentials exhibited by these proteins cannot be attributed to changes in the hydrogen–bonding network surrounding the cluster (Breiter *et al.*, 1991; Rayment *et al.*, 1992). Thus far, refined x-ray coordinates for three plant-type ferredoxins are available, namely those for the vegetative and heterocyst forms of the *Anabaena* protein and for the molecule isolated from *A. sacrum* (Rypniewski *et al.*, 1991; Jacobson *et al.*, 1993b; Tsukihara *et al.*, 1990). In the vegetative and heterocyst forms of the *Anabaena* ferredoxin, the backbone amide hydrogen bonding patterns around the metal clusters are very similar with respect to both bond lengths and overall bond geometry. In the model of the *A. sacrum* ferredoxin, the hydrogen bonding pattern is similar, but the lengths of these putative interactions tend to be longer, as can be seen from Table II. Whether these differences are significant or are merely a result from the *A. sacrum* model being determined to 2.2 Å rather than 1.7 Å resolution is unclear at the present time (Tsukihara *et al.*, 1990).

The refined model of the vegetative *Anabaena* ferrodoxin contains 146 ordered waters, 10 of which are located at identical positions (within 0.20 Å) in the two ferredoxins constituting the asymmetric unit. Eight of these waters lie on the same face of the protein with five forming a channel leading from the interior of the molecule, near the iron-sulfur cluster, to the C-terminal region and the bulk solvent. The

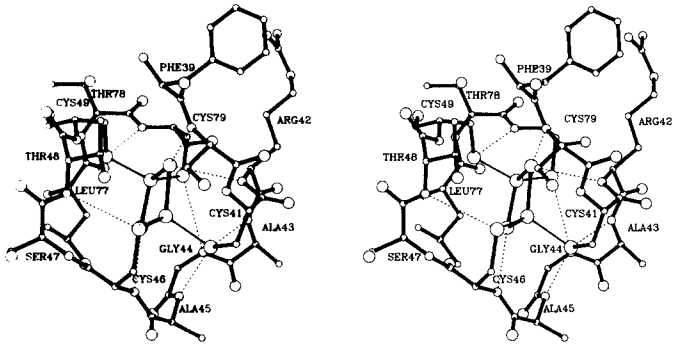

Fig. 7. Stereo view of the vegetative *Anabaena* [2Fe-2S] binding pocket. Those amino acids within approximately 3.5 Å of the metal cluster are shown. The dashed lines indicate the potential hydrogen bonds between backbone amide hydrogens and sulfurs of the cluster or sulfurs of the cysteinyl ligands, 41, 46, and 49.There are no apparent hydrogen bonds to Cys 79.

Table II. Potential Hydrogen Bonds between Sulfur Atoms in the Metal Cluster and Backbone Amide Hydrogens

Atoms involved in H bonds [a]	Distance (Å)			
	Anabaena vegetative FDXN		*Anabaena* heterocyst FDXN	*A. sacrum* FDXN[b]
	Mol I	Mol II		
S1 of Cluster and N of Ser 40	3.4	3.3	3.3	3.2
S1 of Cluster and N of Arg 42	3.2	3.2	3.2	3.8
S2 of Cluster and N of Cys 46	3.3	3.3	3.3	3.2
SG of Cys 41 and N of Ala 43	3.1	3.1	3.2	3.5
SG of Cys 41 and N of Ala 45	3.4	3.4	3.4	3.6
SG of Cys 46 and N of Cys 41	4.0	4.0	4.0	4.8
SG of Cys 46 and N of Thr 48	3.4	3.4	3.4	3.6
SG of Cys 49 and N of Cys 79	3.4	3.4	3.6	3.8

[a] Amino acid residues correspond to the vegetative form of the *Anabaena* ferredoxin.
[b] Distances were measured from the x-ray coordinates obtained from the Brookhaven Protein Data Bank and correspond to the structurally similar amino acid residues of molecule 1 in the *A. sacrum* ferredoxin.

hydrogen-bonding network for these waters is represented schematically in Fig. 8. This water channel is also observed in the refined structure of the ferredoxin from the heterocyst form *Anabaena* 7120 (Jacobson *et al.*, 1993a), but apparently is not present in the structure of the *A. sacrum* ferredoxin (Tsukihara *et al.*, 1990), as determined from the x-ray coordinates deposited in the Protein Data Bank (Bernstein *et al.*, 1977). The biological significance of this water channel is unknown.

The amino acid sequence of *Anabaena* 7120 heterocyst ferredoxin is 51% homologous to that of the vegetative ferredoxin from the same organism and contains the same number of amino acid residues (Böhme and Haselkorn, 1988). In addition, the x-ray

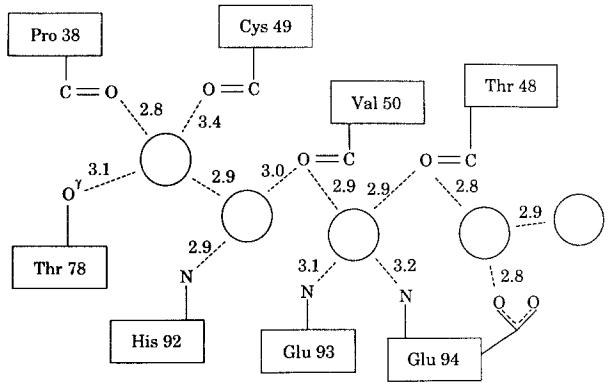

Fig. 8. Schematic representation of the hydrogen bonding pattern displayed by the conserved solvent channel in the *Anabaena* vegetative ferredoxin. The large circles represent ordered solvent molecules. Distances are measured in Ångströms.

model for the heterocyst protein has been determined and refined to 1.7 Å resolution with a crystallographic *R*-value of 16.7% (Jacobson *et al.*, 1993b). The overall secondary structure of the heterocyst molecule consists of five strands of β-pleated sheet, two α-helices, and seven Type I turns. The only significant differences in the polypeptide chain backbone between the *Anabaena* 7120 vegetative and heterocyst ferredoxins occur in the loop delineated by amino acid residues 9–24 and at the three C-terminal residues. The different conformations adopted by these amino acid residues are due to both crystal packing interactions and to amino acid sequence differences. Excluding these regions, the α-carbons for the vegetative and heterocyst ferredoxins superimpose with a root-mean-square deviation of 0.45 Å. A comparison of the *A. sacrum* ferredoxin with the *Anabaena* vegetative ferredoxin reveals 72 structurally equivalent amino acid residues between these two proteins that superimpose with a root-mean-square value of 0.55 Å

In the heterocyst ferredoxin, four of the 22 amino acid positions thought to be conserved in nonhalophilic ferredoxins are not retained (Matsubara and Hase, 1983). Three of these residues, His 42, Ser 43, and Leu 78, are located near the iron-sulfur cluster. In other nonhalophilic ferredoxins these residues are typically arginine, alanine, and threonine, respectively. The other nonconserved residue in the heterocyst ferredoxin is Ala 76, which is typically a valine residue. The arginine-to-histidine replacement in the heterocyst molecule is of special interest in that it was expected that such a change would produce a local rearrangement in the metal binding loop. In fact, the

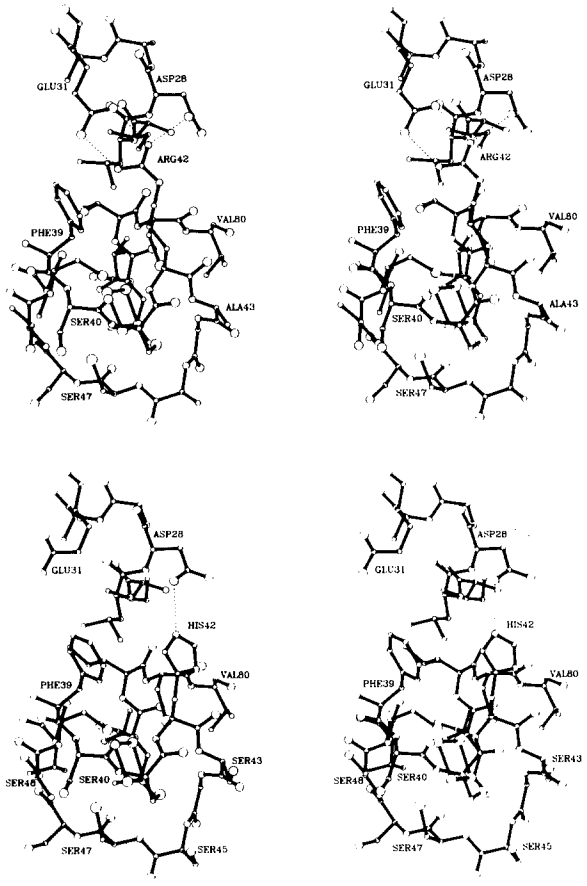

Fig. 9. Comparison of the vegetative and heterocyst ferredoxin structures in the vicinity of amino acid residue 42. (a) In the vegetative ferredoxin, position 42 is an arginine residue which participates in three hydrogen bonds, to Glu 31 and Asp 28, as indicated by the dashed lines. (b) In the heterocyst ferredoxin, residue 42 is a histidine. As shown by the dashed lines, His 42 participates in only one hydrogen bond to Asp 28.

heterocyst and vegetative molecules are very similar in this region, as can be seen in Figs. 9a and 9b. In the vegetative molecule, the guanidino group of Arg 42 is anchored down by three hydrogen bonds to the carboxylates of Glu 31 and Asp 28, whereas in the heterocyst protein, His 42 participates in only one hydrogen bonding interaction, namely that between $N^{\delta 1}$ of the imidazole ring and the carboxylate oxygen of Asp 28. Note that Glu 31 in the heterocyst ferredoxin swings out of the pocket, thereby altering the surface properties of the protein near the vicinity of the [2Fe-2S] cluster. The change from an arginine to a histidine residue with its fewer electrostatic interactions may serve a dual role of modifying both the flexibility of the polypeptide chain and the surface properties of the protein in this region, such as the apparent increased solvent exposure of Leu 27.

One of the striking characteristics of the heterocyst ferredoxin, as compared to the vegetative protein, is the "crown" of serine residues surrounding one side of the iron-sulfur cluster as shown in Fig. 9b. Of the eight serine residues found in the heterocyst protein, five are located in the metal binding loop. The binding pocket is decidedly amphipathic, with one side containing Serines 40, 43, 45, 47, and 48 and the other region lined with hydrophobic residues such as Leu 27, Phe 39, Val 50, Ile 64, Phe 65, Leu 77, Val 78, and Val 80. Fe 1 is located in the hydrophilic portion of the binding pocket, whereas Fe 2 is situated in the more hydrophobic region.

3.2. Crystallization and X-Ray Modeling of Site-Directed Mutants of *Anabaena* 7120 Vegetative Ferredoxin

As discussed above, numerous site-directed mutants of the [2Fe-2S] ferredoxin produced by the vegetative form of *Anabaena* sp. 7120 have been produced in an effort to probe the role of specific amino acid residues in the modulation of oxidation–reduction potentials and electron transfer rates. In terms of their crystallography, these mutants divide into the following two classes.

The first group of mutations, those that change the cysteinyl ligands of the metal center to other amino acids, have yielded proteins whose overall stabilities are decreased by varying degrees. Crystallization attempts for these mutant proteins have been largely unsuccessful. One mutant, that in which Cys 49 was changed to a serine, however, was crystallized. The three-dimensional x-ray structure of this mutant has been determined and refined to 1.7 Å resolution with a crystallographic *R*-factor 18.1%. A possible explanation for the success in crystallizing this particular mutant is that, of the four cysteines ligating the metal center to the protein, only Cys 49 resides in a standard secondary structural element.

Mutants of the second class, those near the iron-sulfur center, have proven much easier to crystallize. X-ray diffraction quality crystals of seven different mutants have been obtained thus far. Three-dimensional models for the mutants, T48S, A50V, A43S, and E94K, have been refined to 1.8 Å resolu-

tion with crystallographic *R*-factors of 17.3, 17.9, 18.0, and 20.3%, respectively. In addition, the structure of a quadruple mutant (A43S/A45S/T48S/A50N) has been completed to 1.8 Å resolution with an *R*-value of 18.3%. An x-ray data set for the mutant S40A has been recently been collected to 1.8 Å resolution, and least-squares refinement of its structure is underway. Details of these mutant structures will be presented elsewhere (Jacobson *et al.*, 1993b).

4. NMR STUDIES OF *ANABAENA* 7120 HETEROCYST AND VEGETATIVE FERREDOXINS IN SOLUTION

NMR spectroscopy provides information complementary to that from x-ray crystallography. The patterns of nuclear Overhauser (NOE) interactions and coupling constants permit the determination of the secondary and tertiary structure in solution, and results from hydrogen exchange and relaxation measurements yield information about the stability or rigidity of particular regions of the protein. With paramagnetic proteins, such as [2Fe-2S] ferredoxins, NMR data provide additional information that is difficult to deduce from other experiments, i.e., the delocalization of unpaired electron density from the iron atoms to individual atoms of the protein and the rates and equilibria of electron exchange reactions. Although it has not proved feasible yet to study reduced [2Fe-2S] ferredoxins by x-ray crystallography, they can be readily reduced in solution and studied by NMR spectroscopy. Thus, it is possible to investigate structural and dynamic changes that accompany oxidation and reduction. Finally, NMR offers the prospect of studying interactions of ferredoxins in solution with their redox partners.

4.1. Assignment Strategies and Stable-Isotope Labeling

NMR assignment strategies for ferredoxins have evolved over the years in response to developments in NMR methodology and in ways of producing and labeling the proteins. Many small proteins ($M_f \leq 12,000$) can be studied in detail at natural abundance by conventional two-dimensional (2D) ^1H NMR methods (Wüthrich, 1986). The inherent paramagnetism of [2Fe-2S] ferredoxins (in both redox states), however, has made it necessary to use more sophisticated approaches. The paramagnetism leads to broadening and shifting of the NMR peaks.

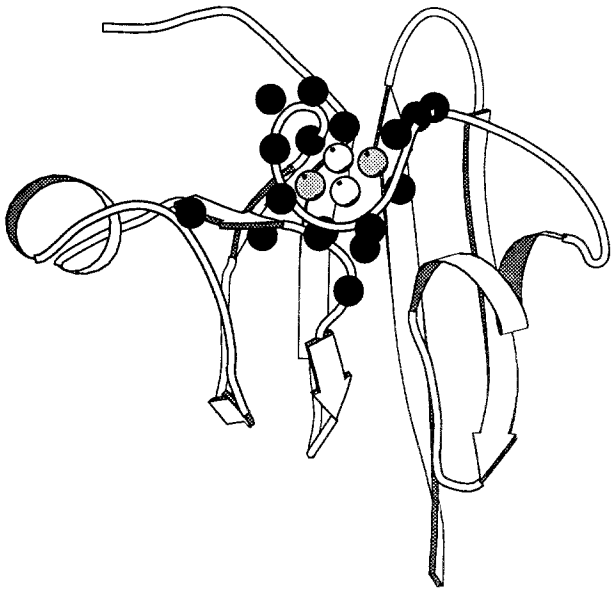

Fig. 10. The black spheres represent the positions of residues in oxidized *Anabaena* 7120 heterocyst ferredoxin whose amide nitrogen signals are missing nD^1H^{15} correlation spectra. The structure shown is a MOLSCRIPT (Kraulis, 1991) representation of the x-ray structure of the oxidized ferredoxin (Jacobson *et al.*, 1993a). The white and gray spheres represent the iron and sulfur atoms, respectively, of the [2Fe-2S] cluster. (Figure from Chae *et al.*, 1993.)

Resonances from protons that have appreciable unpaired electron density are shifted out beyond the diamagnetic envelope, and often are well resolved, although broad. They are relatively easy to detect, but harder to assign because of their faster relaxation that makes it more difficult to establish connectivities to neighboring atoms either *through space* by a nuclear Overhauser (NOE) mechanism or *through bonds* by a spin–spin coupling mechanism. Selective isotopic labeling provides the most secure method for assigning hyperfine-shifted signals (see below).

Signals from protons that are within about 7 Å of the iron-sulfur cluster tend to be broadened beyond detection in normal 2D or 3D NMR experiments (Oh and Markley, 1990a; Chae *et al.*, 1993) (Fig. 10), although they often can be observed in 1D spectra or in specialized 2D experiments such as NOESY with short mixing times (Skjeldal *et al.*, 1991b). Since nuclei with smaller magnetogyric ratios are broadened less, one expects to be able to resolve more ^{13}C and still more ^{15}N signals from atoms near the iron-sulfur cluster (Oh and Markley, 1990b).

Paramagnetic line broadening leads to spectral overlap and makes it more difficult to resolve signals from individual atoms; the loss of signals from resi-

dues close to the iron-sulfur center leads to interruptions in sequential assignment walks. In response to these obstacles, Oh and coworkers developed novel approaches for their studies of the *Anabaena* 7120 vegetative ferredoxin, the first ferredoxin for which extensive assignments were determined (Oh and Markley 1990a,b; Oh *et al.*, 1990). The vegetative ferredoxin was labeled uniformly (to 26%) with ^{13}C, and the ^{13}C spin systems of the amino acid residues were mapped out by a 2D carbon–carbon double-quantum experiment ($^{13}C\{^{13}C\}DQC$) (Oh *et al.*, 1988). The carbon connectivities were then extended to the protons by means of 2D single-bond and multiple-bond $^{1}H\{^{13}C\}$ correlations (Oh *et al.*, 1989). The ^{13}C and ^{1}H spin systems were extended over (one to a few bonds) to neighboring ^{15}N atoms by collecting 2D $^{1}H\{^{15}N\}$ (Oh *et al.*, 1989) and $^{13}C\{^{15}N\}$ data (Mooberry *et al.*, 1989) from proteins labeled with ^{15}N (98%) or ^{15}N (98%) plus ^{13}C (26%). Finally, sequential connectivities were deduced from sequential NOE connectivities derived from standard NOESY spectra or from isotope-filtered 2D NOESY data (Oh and Markley, 1990).

The assignment strategies used to analyze NMR spectra of *Anabaena* 7120 heterocyst ferredoxin (Chae *et al.*, 1993) and human placental ferredoxin (Xia, unpublished) have incorporated modifications that take into account: (1) the different way in which these proteins are being produced (heterologous overproduction in *E. coli* instead of direct isolation from *Anabaena* 7120 as was the case with the vegetative ferredoxin), and (2) the recent introduction and refinement of 3D NMR pulse sequences. Heterologous expression of the protein has led to a large increase in the yield per liter of culture and thus has made it feasible to label the proteins to 99% ^{13}C by growing the cultures on uniformly labeled glucose (instead of the $^{13}CO_2$ substrate used for lower-level labeling with the photosynthetic cyanobacterium) and to label the proteins to 99% with [^{15}N]ammonium sulfate as the nitrogen source (instead of the [^{15}N]ammonium nitrate used with direct protein isolation from *Anabaena*). Overexpression of the protein in *E. coli* has also made it possible to label the protein selectively by feeding ^{15}N- or ^{13}C-labeled amino acid residues as precursors. It has been advisable in some cases, for example, when labeling cysteines or histidines, to use auxotrophic strains of *E. coli* to ensure that the label is not lost or transferred to other amino acids.

Despite the advances these methods offer, the intrinsic paramagnetism of the protein has impeded to date the full assignment of any [2Fe-2S] ferredoxin. Assignment of the diamagnetic signals from residues beyond 7 Å of the irons is now relatively straightforward, and one can determine the structure of the protein surrounding the cluster. Of course, the NMR signals of the remaining residues are of particular interest since they report on the active site. Steady progress is being made in assignments of the hyperfine-shifted ^{1}H (Chan and Markley, 1983), ^{13}C (Chan and Markley, 1983), and ^{15}N (Oh and Markley, 1990b) signals of [2Fe-2S] ferredoxins. A breakthrough in assigning the hyperfine ^{1}H NMR peaks came with realization that the nuclear Overhauser effect (NOE) could be employed, provided that the mixing times are short. Dugad *et al.* (1990) used one-dimensional NOE's to partially assign the hyperfine spectrum of reduced spinach and *S. platensis* ferredoxins with reference to the x-ray structure of *S. platensis* ferredoxin. Skjeldal *et al.* (1991b) extended this approach to two-dimensional NOE spectroscopy and used the more highly refined structure of the *Anabaena* 7120 vegetative ferredoxin (Rypniewski *et al.*, 1991) to obtain nearly complete hyperfine ^{1}H assignments of the reduced form of that protein. Moreover, it was found that the assignments could be extended to the oxidized form of the ferredoxin by magnetization transfer (Skjeldal *et al.*, 1991b). Many of these ^{1}H assignments have been confirmed recently by selective isotopic labeling and have been extended by a novel NMR approach to hyperfine-shifted ^{15}N and ^{13}C signals (Cheng *et al.*, 1993a). Similar approaches are being used to assign the hyperfine-shifted resonances of the *Anabaena* 7120 heterocyst and human ferredoxins. New approaches may be required in order to assign all the remaining resonances, including those that are hyperfine shifted and those that are broadened by paramagnetic or exchange mechanisms.

4.2. Current Status of Our NMR Studies of [2Fe-2S] Ferredoxins

Single (^{15}N) and double (^{15}N and ^{13}C) labeled samples have been prepared of wild-type, recombinant human ferredoxin, heterocyst *Anabaena* 7120 ferredoxin, and vegetative *Anabaena* 7120 ferredoxin. In addition, a number of selectively labeled samples of each protein have also been made. Nearly complete ^{1}H, ^{13}C, and ^{15}N assignments are available now for the diamagnetic backbone atoms of the vege-

tative (Oh and Markley, 1990a; Oh *et al.*, 1990) and heterocyst (Chae *et al.*, 1993) *Anabaena* 7120 ferredoxins in their oxidized states. More extensive side chain assignments have been determined for the vegetative ferredoxin than for the heterocyst. Multinuclear, multidimensional NMR data for the reduced forms of these proteins are being collected. The limited stability of the ferredoxins over time (particularly the heterocyst ferredoxin) has precluded the successful collection of 4D NMR data sets which require up to four days. (Denaturation of even a small amount of protein leads to the release of sufficient iron to cause spectral degradation.) It has been possible, however, to collect 2D and 3D data sets.

Mutagenesis and multinuclear NMR studies have been used to assign the histidine imidazole ^{1}H, ^{13}C, and ^{15}N resonances of human ferredoxin (Xia *et al.*, 1993). Similarities between the aromatic region of human ferredoxin (Xia *et al.*, 1993) and other vertebrate ferredoxins (adrenodoxins) (Miura and Ichikawa, 1991a,b) indicate that the structures of these proteins must be very similar. More extensive assignments of human ferredoxin are under way.

By comparing x-ray and NMR data on the vegetative *Anabaena* 7120 ferredoxin, we obtained nearly complete assignments for the hyperfine proton resonances. After assigning signals to the cysteines, an additional spin system was left over. These signals were assigned tentatively to Arg^{42} (Skjeldal *et al.*, 1991b), but the assignment needs to be verified by selective deuterium labeling (work in progress). Residue 42 is strictly conserved as arginine in all photosynthetic ferredoxins whose sequences we know about. By contrast, the homologous residue in *Anabaena* heterocyst ferredoxin and putidaredoxin is a histidine, and that in the vertebrate ferredoxins is a glutamate (see Fig. 1). When the single arginine of the vegetative ferredoxin was labeled selectively with ^{15}N, its hyperfine-shifted backbone ^{15}N signal was resolved in the oxidized state but not in the reduced state of the protein (Cheng *et al.*, 1993a). This result is consistent with the existence of the hydrogen bond to Arg 42 in both the oxidized and reduced forms of the protein (x-ray data on this point are available only from the oxidized protein; Rypniewski *et al.*, 1991). Further evidence for unpaired spin density on nitrogen was provided by ENDOR studies (Houseman *et al.*, 1992) of the vegetative *Anabaena* 7120 ferredoxin at natural abundance and labeled uniformly with ^{15}N and ^{13}C. The results showed that this ferredoxin has an unusually large nitrogen-electron coupling, $A(^{14}N) = 4\,MHz$. From comparison with the x-ray structure and the NMR results, it was suggested that it is the amide nitrogen from Arg 42; again, the assignment needs to be verified by ENDOR examination of the sample labeled selectively by incorporation of [^{15}N]arginine.

We have studied electron self-exchange in [2Fe-2S] ferredoxins. Magnetization transfer studies have enabled cross-assignment of signals from oxidized and reduced *Anabaena* 7120 photosynthetic ferredoxin (Skjeldal *et al.*, 1991b). The self-exchange rate, which is slow on the NMR time scale of the hyperfine resonances, can be speeded up by addition of a redox reagent such as methyl viologen (Skjeldal *et al.*, 1990).

4.3. NMR Structural Data and Comparison with X-Ray Results

Low-resolution structures of the *Anabaena* 7120 vegetative and heterocyst ferredoxins have been determined from their NMR data by restrained molecular dynamics (Y. K. Chae, B.-H. Oh, and J. L. Markley, unpublished results). These models have incorporated the pattern of cysteine ligation to the [2Fe-2S] clusters determined from the x-ray results. Because of the lack of information from residues close to the iron atoms, the peptide loop that surrounds the cluster is very poorly defined. In other regions, it has been possible to use evidence from NOEs and chemical shifts to compare the structures to one another and to the corresponding x-ray structures (Chae *et al.*, 1993).

There is general agreement between the NMR and x-ray data in terms of the secondary structural elements and overall fold of these proteins. Most of the differences in NMR parameters for corresponding atoms in the vegetative and heterocyst ferredoxins can be rationalized in terms of local structural differences seen in the crystal structures. Figure 11a compares the chemical shifts of the alpha protons of the two proteins (Chae *et al.*, 1993). The largest differences are seen in the N-terminal half of the molecule, particularly residues 9–24 where the x-ray structures show a large difference in the orientation of the polypeptide backbone.

Figure 11bc compares the chemical shift indices (Wishart *et al.*, 1992) for the two proteins (Chae *et al.*, 1993) which can be interpreted in terms of secondary structure. A dense region (3 or more in a row) of "−1" means a helix; a dense region of "+1" means an extended conformation. Regions in which "+1" and

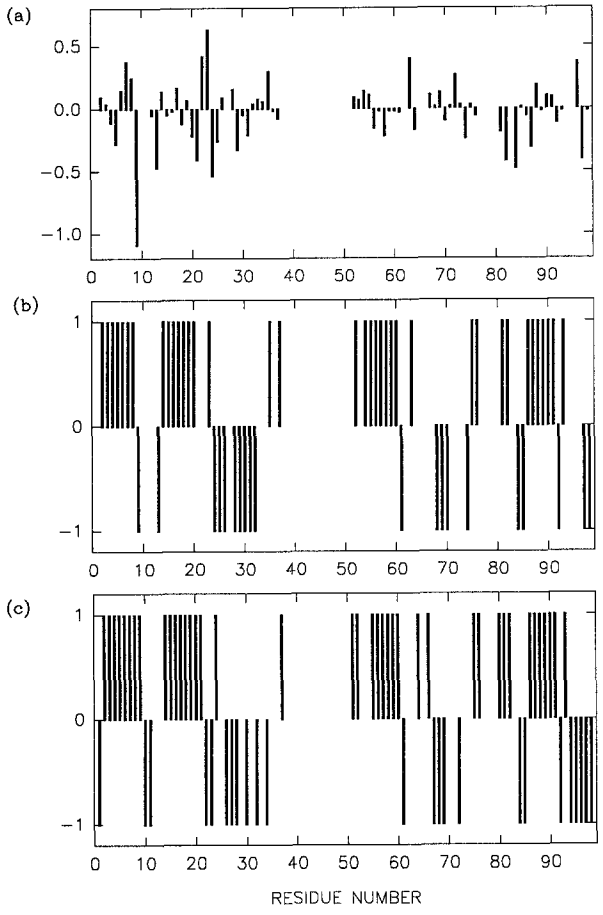

Fig. 11. Comparison of the ^{1}H NMR chemical shifts of the alpha protons of the vegetative and heterocyst ferredoxins (oxidized) from *Anabaena* 7120. (a) Chemical shift differences of residues whose signals have been resolved and assigned ($\delta_{\text{heterocyst}} - \delta_{\text{vegetative}}$); in cases where the residue is not conserved, the chemical shifts have been corrected for intrinsic (amio acid specific) differences. Conversion of alpha proton chemical shifts into the "chemical shift index" of Wishart *et al.* (1992): (b) vegetative ferredoxin and (c) heterocyst ferredoxin. As discussed in the text, these patterns provide an indication of the secondary structural features of the proteins in solution. (Figure from Chae *et al.*, 1993.)

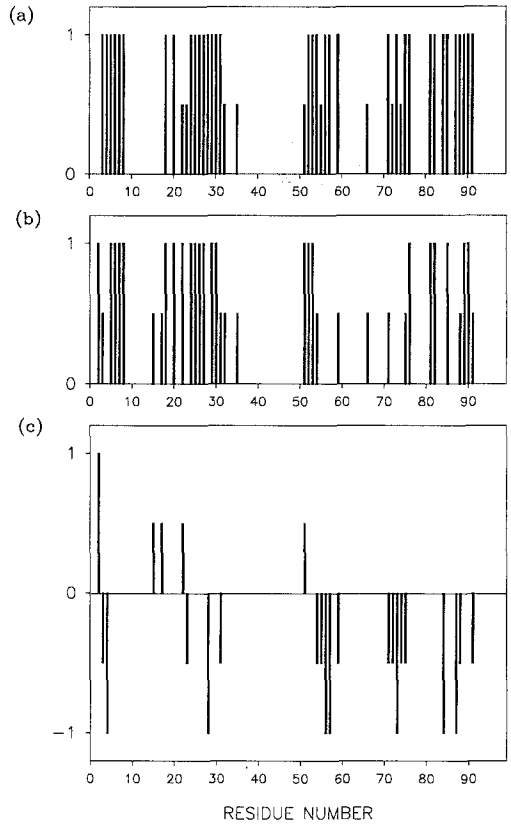

Fig. 12. Schematic depictions of the backbone amide proton exchange rates of *Anabaena* 7120 ferredoxins: (a) vegetative ferredoxin, (b) heterocyst ferredoxin, (c) exchange rate differences between the two, $\text{rate}_{\text{heterocyst}} - \text{rate}_{\text{vegetative}}$. This figure provides only qualitative estimates of the exchange rates: "1.0" indicates protection of the amide proton from exchange for over 30 h; "0.5" indicates protection of the amide proton for 8 h but less than 30 h. The data indicate that the structure of the vegetative ferredoxin is considerably more rigid than that of the heterocyst ferredoxin. (Figure from Chae *et al.*, 1993.)

"−1" alternate ("−1 + 1" or "+1 − 1") show a partial correlation with turns (Wishart *et al.*, 1992). The results shown in Fig. 11bc indicate that the two proteins have very similar patterns of secondary structure. This conclusion is reinforced by NOE data (not shown).

The most remarkable difference between the vegetative and heterocyst ferredoxins, as revealed by NMR spectroscopy, is in their rigidity. Although the differences in stability are reflected in the patterns of chemical shifts and NOEs, they are seen most clearly from hydrogen exchange data. Figure 12 shows a very qualitative comparison of the hydrogen exchange rates of the two proteins.

The NMR data indicate that Lys 10 and Lys 11 are part of a very flexible loop in the heterocyst ferrodoxin (Chae *et al.*, 1993), whereas the corresponding residues of the vegetative ferredoxin are part of a β-turn (Oh and Markley, 1990a). Although the x-ray structures show that residue 10 has different hydrogen bonding partners in the two proteins (Jacobson *et al.*, 1993), the x-ray structure of the heterocyst ferredoxin shows that residues 10–13 are ordered in a Type-I turn. NMR evidence for disorder at residues 10 and 11 of the heterocyst ferredoxin comes from the lack of NOE build-up from their protons. The Type -I turn observed in the x-ray structure may not be present when the protein is in solution.

In the second half of the sequence, large chemical shift differences for the two ferredoxins are observed only in the region between residues 83 and 88 and in the C-terminal residues (Fig. 11a). According to the chemical shift index analysis (Fig. 11bc), residues 80–85 appear to be more extended in the heterocyst ferredoxin and more helical in the vegetative ferredoxin. The NMR results are in agreement with the x-ray structures which show that the fifth β-strand is continuous through residues 82–91 in the vegetative ferredoxin but that it is interrupted in the heterocyst ferredoxin such that only residues 81–83 and 87–91 are helical (Jacobson *et al.*, 1993a). Since these residues are close to the [2Fe-2S] cluster, these structural differences may play a functional role. The chemical shift differences observed at the C-terminus also are consistent with structural differences observed in the x-ray structures. The substitution of Glu 95 (vegetative Fd) for Pro 95 (heterocyst Fd), which promotes a tight turn, appears to convert the helical turn seen in the vegetative ferredoxin to the Type I turn seen in the heterocyst ferredoxin (Jacobson *et al.*, 1993a).

4.4. Classification of [2Fe-2S] Ferredoxins on the Basis of Their Hyperfine Shifts

Ferredoxins can be classified into two general categories on the basis of hyperfine proton chemical shifts (particularly of the reduced proteins) (Skjeldal *et al.*, 1991a). One category includes the plant-type ferredoxins as exemplified by the vegetative and heterocyst ferredoxins of *Anabaena* 7120. In this class, all signals from the cysteine ligands of the reduced proteins are shifted well downfield (+120 ppm); signals from cysteines ligated to Fe(III) exhibit Curie-type temperature dependence, and those from cysteines ligated to Fe(II) exhibit anti-Curie-type temperature dependence (Dugad *et al.*, 1990; Skjeldal *et al.*, 1991b). The other category includes the vertebrate-type ferredoxins (Skjeldal *et al.*., 1991a) and *E. coli* ferredoxin (L. Skjeldal, L. E. Vickery, and J. L. Markley, unpublished data). In their reduced state, hyperfine proton signals are found both upfield (−2 to −18 ppm) and downfield (+15 to +45 ppm), and all exhibit Curie-type temperature dependence.

The different patterns of hyperfine shifted peaks observed in photosynthetic and mitochondrial ferredoxins appear to arise from differences in Fermi contact coupling and magnetic susceptibility. They are correlated with differences in the anisotropy of the electronic g-tensor: photosynthetic ferredoxin, rhombic; mitochondrial ferredoxin, axial.

4.5. NMR Studies of Mutant Ferredoxins

Although the primary protein ligands to the iron-sulfur clusters of all known ferredoxins are cysteine sulfurs, non-cysteine ligands have been found in other [2Fe-2S] protein classes: the nitrogens of two histidine imidazoles in the case of Rieske-type proteins (Gurbiel *et al.*, 1991) or oxygen as in the iron-sulfur cluster of aconitase (Robbins and Stout, 1989). Werth *et al.* (1990) have mutated to serine all four N-terminal cysteine residues in the FrdB subunit of *E. coli* fumarate reductase which participate in a [2Fe-2S] cluster. The results indicated that [2Fe-2S] clusters can be assembled with sulfurs from three cysteine and an oxygen ligand from one serine. Potential non-cysteine ligands in [4Fe-4S] model compounds have been studied by Evans and Leigh (1991); their results suggest that the pK_a of the group is a major factor in determining whether a group is a potential donor: the pK_a should be less than 13.6. The pK_a of the cysteine SH is about 9; the pK_a of the serine OH is 13.6, and that of tyrosine is 10. A larger NMR hyperfine interaction has been found for anionic oxygen-cluster binding that for sulfur-cluster binding in these model compounds; in these model compounds, the sense of the temperature dependence of the hyperfine chemical shifts is reversed for serinato-complexes or tyrosinato-complexes compared to cysteinato-complexes.

Clearly, it is of interest to investigate potential non-cysteine ligands in ferredoxins by mutagenesis. We have begun by mutating the four cysteine residues of *Anabaena* 7120 vegetative ferredoxin (Cys 41, Cys 46, Cys 49, Cys 79) into serines (Cheng *et al.*, 1993b). The UV-VIS spectra of these mutant proteins are all different from the wild-type protein. The patterns of hyperfine proton shifts of the mutants also differ from those of the wild-type protein (Fig. 13). Selective isotopic labeling is being used to assist in the assignment of the hyperfine signals of these mutant proteins. Figure 14 (bottom) shows the ^{1}H NMR spectrum of the reduced Cys 46 → Ser mutant. The signals from the three cysteine and one serine ligand have been distinguished by selective deuterium labeling (Fig. 14, top). The reduced state hyperfine shifts of its cysteines are larger than the corresponding ones of the wild-type protein. The temperature dependence

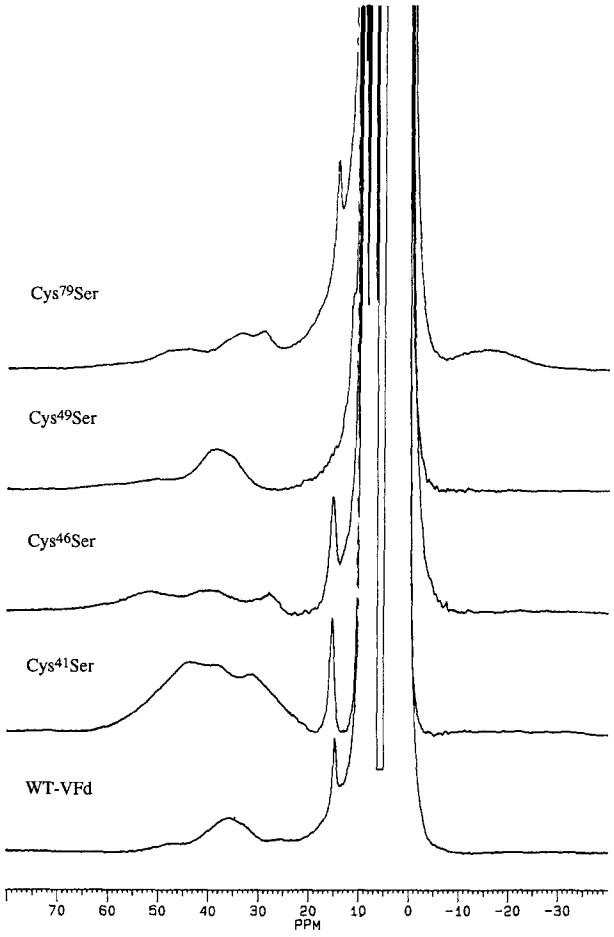

Fig. 13. Comparison of the hyperfine ^{1}H NMR signals from residues ligated to the [2Fe-2S] clusters of wild-type vegetative ferredoxin (WT-VFd) and the four Cys → Ser mutants ($Cys^{41}Ser$, $Cys^{46}Ser$, $Cys^{49}Ser$, and $Cys^{79}Ser$). The different patterns of hyperfine shifts demonstrate that sulfur-to-oxygen substitutions at different cluster ligation positions leads to large differences in electron delocalization. (Figure from Cheng *et al.*, 1993b.)

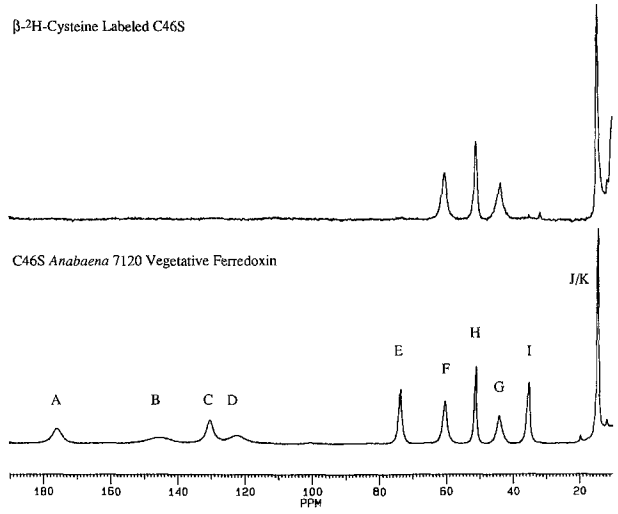

Fig. 14. Pattern of hyperfine ^{1}H NMR peaks from a reduced mutant *Anabaena* 7120 vegetative ferredoxin, $Cys^{46}Ser$ (C46S). The bottom spectrum of the protein at natural isotopic abundance. The top spectrum is of a protein sample in which the cysteines have been labeled with deuterium at the beta positions. By comparison of the top and bottom spectra, peaks A, B, C, D, E, and I can be assigned to the six beta protons of the cysteines (two on each cysteine). Peaks F and G are assigned to the beta protons of Ser^{46}, and peak H is assigned to the alpha proton of Ser^{46}. The sample contained ~ 4 mM protein in 100 mM sodium pyrophosphate buffer and 100 mM sodium chloride. The pH* (uncorrected glass-electrode pH meter reading) was 8.5. Each sample was reduced by addition of ~ 2 mg solid sodium dithionite under argon. The spectra were recorded at a temperature of 298 K with an NMR spectrometer with a proton frequency of 400 MHz (Bruker AM-400). (Figure from Cheng *et al.*, 1993b.)

of these hyperfine shifts (not shown) shows that Cys 41 and Ser 46 are ligated to Fe(II) and that Cys 49 and Cys 79 are ligated to Fe (III) (Cheng *et al.*, 1993b); thus the sulfur-to-oxygen substitution at the γ-atom of residue 46 does not alter which iron is reduced.

5. FUNCTIONAL STUDIES

We have used site-directed mutagenesis to characterize the structural determinants of the interaction of the *Anabaena* 7120 vegetative ferredoxin with both physiological and nonphysiological reaction partners. In as much as previous binding and kinetic studies of the interaction of ferredoxins with ferredoxin $NADP^+$ reductase (FNR) (Walker *et al.*, 1990, 1991; Gomez-Moreno, 1987; Zanetti and Merati, 1987; Hervas *et al.*, 1992) indicated a strong electrostatic component involving acidic residues in ferredoxin and basic residues in FNR, one goal of our structure/function studies was to explore the role of specific charged side chains in both recognition and electron transfer (ET). A second goal was to identify other kinds of amino acid side chains (e.g., aromatic or polar uncharged residues) which might also be involved in these processes. We have utilized laser flash photolysis/time-resolved absorption spectroscopy to investigate the transient kinetics of the oxidation of reduced ferredoxin by its physiological redox partner FNR (isolated from the closely related cyanobacterium *Anabaena* PCC 7119), and the reduction of ferredoxin by the nonphysiological reagent, 5-deazariboflavin semiquinone ($dRfH^\bullet$). The mutations have been made in several conserved aspartates and glutamates (charge reversal to lysine), in a conserved

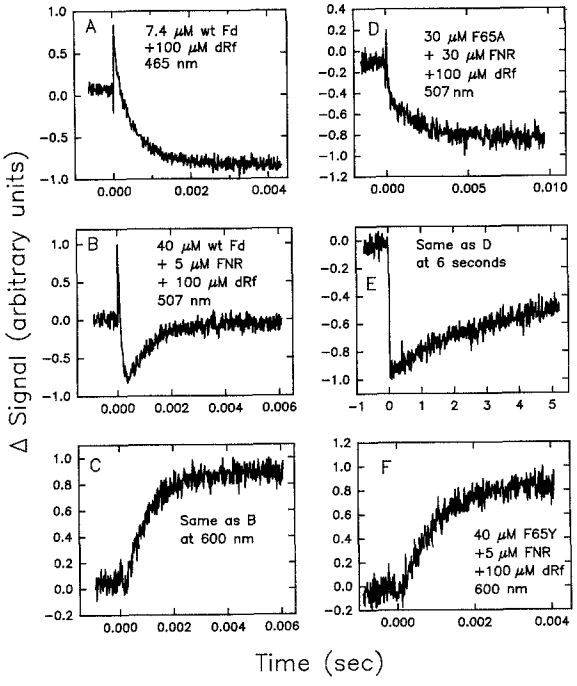

Fig. 15. Transient decay curves of dRf/EDTA solutions containing wt Fd plus or minus FNR, and F65A or F65Y mutant Fds plus FNR at the monitoring wavelengths and concentrations indicated. Solutions also contained 1 mM EDTA in 4 mM phosphate buffer, pH 7.0. Ionic strength was 12 mM. Note that the trace in panel E is on a 5-sec time scale whereas the others are on millisecond time scales.

arginine residue (changed to alanine and to histidine), in a conserved phenylalanine residue (changed to alanine, to isoleucine, to tryptophan, and to tyrosine), and in a partially conserved threonine residue (changed to alanine).

The laser flash photolysis apparatus used to monitor these reactions (Przysiecki *et al.*, 1985; Bhattacharyya *et al.*, 1983), and the methods of data analysis and interpretation (Tollin and Hazzard, 1991; Cusanovich, 1991; Tollin *et al.*, 1993) have been described previously. Briefly, laser flash photolysis of a dRf/EDTA solution produces dRfH$^{\bullet}$, which reduces oxidized protein in competition with its own disproportionation. All kinetic experiments (done anaerobically) were performed under pseudo-first order conditions, with protein being present in large excess over the photogenerated dRfH$^{\bullet}$ (see Hurley *et al.*, 1993a for further details).

Upon laser flash photolysis of dRf/EDTA solutions containing oxidized, recombinant wt Fd, a kinetic trace such as that shown in Fig. 15a is obtained. This transient shows a rapid increase in

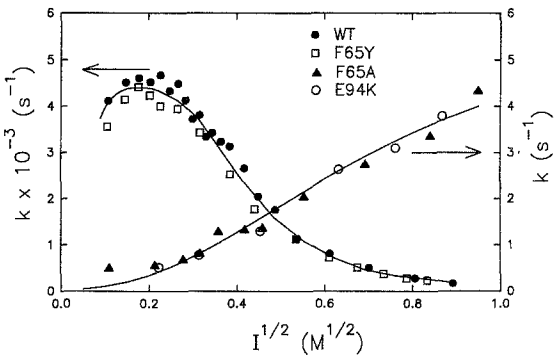

Fig. 16. Ionic strength dependence of observed pseudo-first order rate constants for FNR reduction by wt and mutant Fds. Solutions contained 40 μM Fd and 40 μM FNR, except for wt Fd which was 30 μM in each protein. Decays were monitored at 600 nm for wt and F65Y and at 507 nm for F65A and E94K. Other conditions were as in Fig. 15.

absorbance due to dRfH$^{\bullet}$ production, followed by an exponential decay to below the preflash baseline due to electron transfer from dRfH$^{\bullet}$ to ferredoxin, which results in a loss of absorption at this wavelength. By monitoring this decay as a function of FNR concentration (not shown), a second-order rate constant for the reaction of wt Fd with dRfH$^{\bullet}$ of $2.2 \pm 0.2 \times 10^8\ M^{-1}\ s^{-1}$ is obtained (Table I). All mutant ferredoxins studied thus far have rate constants for this reaction which are within a factor of 2 of the wt value (Table I), indicating that none of the mutations seriously perturb the ability of the Fe/S cluster to accept an electron. This rate constant value also is consistent with that reported previously (Walker *et al.*, 1991) for the similar reaction with the ferredoxin isolated from *Anabaena* 7119 which was carried out under similar conditions ($1.60 \pm 0.2 \times 10^8\ M^{-1}\ s^{-1}$).

When FNR is present, reduced ferredoxin is reoxidized by FNR as shown by the kinetic traces in Fig. 15b,c [measured at an FNR isobestic point (b) and at a wavelength characteristic of reduced FNR (c), both with identical kinetics], consistent with the earlier results (Walker *et al.*, 1991). The variation of k_{obs} with FNR concentration yields a second-order rate constant for the reduction of FNR by reduced wt Fd of $1.2 \pm 0.1 \times 10^8\ M^{-1}\ s^{-1}$ (Table I). This value reflects both complex formation and intracomplex ET processes (Hurley *et al.*, 1993a).

The majority of the mutant ferredoxins studied thus far have shown wild-type behavior ($k = 1$–$2 \times 10^8\ M^{-1}\ s^{-1}$) for ET from reduced ferredoxin to FNR (Table I). In sharp contrast, mutants F65A,

F65I, S64Y/F65A, E94K, and E94K/E95K had ET rate constants which were four orders of magnitude smaller than that for wt Fd. Figure 15d,e shows kinetic traces for the reduction of F65A by dRfH$^{\cdot}$ and for the reduction of FNR by the reduced ferredoxin mutant. Although small but significant decreases in complex stability were observed between these oxidized mutant ferredoxins and oxidized FNR (Table I), these changes were clearly not large enough to account for the kinetic effects, suggesting that the electron transfer process is also being modulated by these mutations (Hurley *et al.*, 1993a). Especially noteworthy is that mutation at Glu 95, which is adjacent to the crucial Glu 94 residue, also resulted in wild-type behavior (Table I). This dramatic difference suggests a very precise surface complementarity at the protein–protein interface. Similarly, the results with mutations at Arg 42, Thr 48, Asp 68, and Asp 69 support the involvement of a highly restricted region of the ferredoxin surface in the FNR interaction domain. An analogous high level of structural specificity has also been observed in several other protein ET systems (Mauro *et al.*, 1988; Coghlan and Vickery, 1992).

It is also important to note that the F65W and F65Y mutants were similar to wt Fd with regard to their reactivities with both dRfH$^{\cdot}$ and FNR, whereas the double mutant S64Y/F65A, which places an aromatic residue adjacent to position 65, has properties analogous to F65A (Hurley *et al.*, 1993b; Table I). Figure 15f shows a kinetic trace for the reduction of FNR by reduced F65Y. These results clearly demonstrate that *Anabaena* 7120 ferredoxin requires an aromatic amino acid at position 65 for efficient ET to FNR.

Steady-state experiments have demonstrated that the *Anabaena* 7120 heterocyst ferredoxin is active in $NADP^+$ photoreduction with an *in vitro* system (Schrautemeier and Böhme, 1985). Consistent with this, we find that the heterocyst ferredoxin reacts with both dRfH$^{\cdot}$ and FNR with rate constants comparable to those of the wild-type vegetative ferredoxin, and that the two proteins have similar redox potentials when measured under similar conditions (Table I). The heterocyst ferredoxin differs from the vegetative ferredoxin in that Glu 95 is replaced by Pro, Thr 48 by Ser, and Arg 42 by His; however, both Phe 65 and Glu 94 are conserved. Thus, the activity of both ferredoxins is consistent with the results from site-directed mutagenesis studies, and further indicate that residue 98, which is a tyrosine in the vegetative ferredoxin but is an alanine in the heterocyst ferredoxin, also is not a crucial residue for ET to FNR.

We have also examined the effect of ionic strength in the reduction of FNR by wt Fd and several mutant ferredoxins (Fig. 16). The increase in k_{obs} in the low ionic strength region with wt Fd has been observed previously for the *Anabaena* 7119 proteins (Walker *et al.*, 1991), and has also been seen in other protein–protein ET systems (Meyer *et al.*, 1993; Hazzard *et al.*, 1988, 1991). This effect has been attributed to a situation in which the most stable complex at low ionic strength is not optimal for electron transfer, and that some "loosening" of the complex is necessary to allow the two proteins to assume a mutual orientation that is more favorable to ET.

Those mutants that showed wild-type behavior in their reaction with FNR (see Table I) showed ionic strength dependence similar to that of wt Fd. In marked contrast, F65A, F65I, S64Y/F65A, and E94K showed dramatically different dependence (cf. Fig. 16). A possible explanation for this result is that the orientation of the proteins within the ET complex at all ionic strengths is so far from optimal with these mutants that any "loosening" by salt addition allows them to assume an orientation that is more favorable for electron transfer. It is important to note that replacement of Phe 65 by another aromatic residue restores wild-type behavior with respect to ionic strength (shown for F65Y in Fig. 16).

Although Glu 94 is clearly crucial to an effective ET interaction with FNR, its precise role is not clear at present. Future studies with other mutations should help to delineate this (e.g., E94Q, E94D). We are also planning experiments to determine if other residues close to Glu 94 and Phe 65 (e.g., Ser 47, Asp 67), or if other conserved charged residues (e.g., Glu 31, Glu 32), are important in the protein–protein interaction.

We have also studied the reactivity of the mutants in which each of the four cysteines that ligate the [2Fe-2S] cluster have been changed to serines (i.e., C41S, C46S, C49S, and C79S). Preliminary measurements on the first three of these mutants indicate that they react normally with dRfH$^{\cdot}$ and that they do participate in ET to FNR. Details of these studies will be published elsewhere.

Finally, it is important to know whether or not the same ferredoxin residues that critically modulate ferredoxin/FNR electron transfer are also crucial to electron transfer from Photosystem I to ferredoxin. Experiments designed to determine this are in progress.

ACKNOWLEDGMENT

This work was supported by grants from the National Institutes of Health (GM30982 to H.M.H., DK15057 to G.T.), National Science Foundation (MCB-9215142 to J.L.M.), U.S. Department of Agriculture (USDA/SEA #9200684 to J.L.M.), and CAICYT (BI091-1124-CO2-01 to G.T.). NMR studies were carried out in the National Magnetic Resonance Facility at Madison which is supported by NIH grant RR02301. Equipment in the NMR Facility was purchased with funds from the NIH Biomedical Research Technology Program (grant RR02301), the University of Wisconsin, the NSF Biological Instrumentation Program (grant DMB-8415048), the NIH Shared Instrumentation Program (grant RR02781), and the U.S. Department of Agriculture.

REFERENCES

Alam, J., Whitaker, R. A., Krogmann, D. W., and Curtis, S. E. (1986). Isolation and sequence of the gene for ferredoxin I from the cyanobacterium *Anabaena* sp. strain PCC 7120, *J. Bacteriol.* **168**, 1265–1271.

Ausubel, F. M., Brent, R., Kingston, R. E., Moore, D. D., Seidman, J. G., Smith, J. A., and Struhl, K. (eds.) (1989). *Current Protocols in Molecular Biology*, Wiley, New York.

Backes, G., Mino, Y., Loehr, T. M., Meyer, T. E., Cusanovich, M. A., Sweeney, W. V., Adman, E. T., and Sanders-Loehr, J. (1991). The environment of Fe_4S_4 clusters in ferredoxins and high-potential iron proteins. New information from x-ray crystallography and resonance Raman spectroscopy, *J. Am. Chem. Soc.* **113**, 2055-2064.

Barker, W. C., George, D. G., Srinivasarao, G. Y., and Yeh, L. S. (1992). Database of protein sequence alignments, *Biophys. J.* **61**, A348 (Abstract #2000).

Bernstein, F. C., Koetzle, T. F., Williams, G. J. B., Meyer, E. F., Jr., Brice, M. D., Rogers, J. R., Kennard, O., Shimanouchi, T., and Tasumi, M. (1977). The protein data bank: a computer-based archival file for macromolecular structures, *J. Mol. Biol.* **112**, 535–542.

Bhattacharyya, A. K., Tollin, G., Davis, M., and Edmondson, D. E. (1983). Laser flash photolysis studies of intramolecular electron transfer in milk xanthine oxidase, *Biochemistry* **22**, 5270–5279.

Böhme, H., and Haselkorn, R. (1988). Molecular cloning and nucleotide sequence analysis of the gene coding for heterocyst ferredoxin from the cyanobacterium *Anabaena* sp. strain PCC 7120, *Mol. Gen. Genet.* **214**, 278–285.

Böhme, H., and Haselkorn, R. (1989). Expression of *Anabaena* ferredoxin genes in *Escherichia coli*, *Plant Mol. Biol.* **12**, 667–672.

Böhme, H., and Schrautemeier, B. (1987). Comparative characterization of ferredoxins from heterocysts and vegetative cells of *Anabaena variabilis*, *Biochim. Biophys. Acta* **891**, 1–7.

Breiter, D. R., Meyer, T. E., Rayment, I., and Holden, H. M. (1991). The molecular structure of the high-potential iron-sulfur protein isolated from *Ectothiorhodospira halophila* determined at 2.5 Å resolution, *J. Biol. Chem.* **266**, 18660–18867.

Chae, Y. K., Abildgaard, F., Mooberry, E. S., and Markley, J. L. (1993). Multinuclear, multidimensional NMR studies of *Anabaena* 7120 heterocyst ferredoxin. Sequence-specific resonance assignments and secondary structure in solution of the oxidized form, *Biochemistry*, submitted.

Chan, T.-M., and Markley, J. L. (1982). Heteronuclear (^1H, ^{13}C) two-dimensional chemical shift correlation NMR spectroscopy of a protein. Ferredoxin from *Anabaena variabilis*, *J. Am. Chem. Soc.* **104**, 4010–4011.

Chan, T.-M., and Markley, J. L. (1983). Nuclear magnetic resonance studies of two-iron-two-sulfur ferredoxins. 5. Hyperfine-shifted peaks in ^1H and ^{13}C spectra, *Biochemistry* **22**, 6008–6010.

Chan, T.-M., Hermodson, M. A., Ulrich, E. L., and Markley, J. L. (1983a). Nuclear magnetic resonance studies of two-iron-two-sulfur ferredoxins. 2. Determination of the sequence of *Anabaena variabilis* ferredoxin II, assignment of aromatic resonances in proton spectra, and effects of chemical modifications, *Biochemistry* **22**, 5988–5995.

Chan, T.-M., Ulrich, E. L., and Markley, J. L. (1983b). Nuclear magnetic resonance studies of two-iron-two-sulfur ferredoxins. 4. Interactions with redox partners. *Biochemistry* **22**, 6002–6007.

Cheng, H., Westler, W. M., Xia, B., Oh, B.-H., and Markley, J. L. (1993a). Protein expression, selective isotopic labeling, and analysis of hyperfine-shifted NMR signals of *Anabaena* 7120 vegetative [2Fe-2S] ferredoxin, in preparation.

Cheng, H., Xia, B., Reed, G. H., and Markley, J. L. (1993b). Optical, EPR and ^1H NMR spectroscopy of serine-ligated [2Fe-2S] ferredoxins produced by site-directed mutagenesis of cysteine residues in recombinant *Anabaena* 7120 vegetative ferredoxin, *Biochemistry*, submitted.

Coghlan, V. M., and Vickery, L. E. (1989). Expression of human ferredoxin and assembly of the iron-sulfur center in *Escherichia coli*. *Proc. Natl. Acad. Sci. USA* **86**, 835–839.

Coghlan, V. M., and Vickery, L. E. (1991). Site-specific mutations in human ferredoxin that affect binding to ferredoxin reductase and cytochrome P450*scc*, *J. Biol. Chem.* **266**. 18606–18612.

Coghlan, V. M., and Vickery, L. E. (1992). Electrostatic interactions stabilizing ferredoxin electron transfer complexes. Distribution by "conservative" mutations, *J. Biol. Chem.* **267**, 8932–8935.

Cupp, J. R., and Vickery, L. E. (1988). Identification of free and $[Fe_2S_2]$-bound cysteine residues of adrenodoxin, *J. Biol. Chem.* **263**, 17418–17421.

Cusanovich, M. A. (1991). Photochemical initiation of electron transfer reactions. *Photochem. Photobiol.* **53**, 845–857.

Cushman, D. W., Tsai, R., and Gunsales, I. C. (1967). The ferroprotein component of a methylene hydroxylase, *Biochem. Biophys. Res. Commun.* **26**, 577–583.

Deng, W. P., and Nickoloff, J. A. (1992). Site-directed mutagenesis of virtually any plasmid by eliminating a unique site, *Anal. Biochem.* **200**, 81–88.

Dugad, L. B., Le Mar, G. N., Banci, L., and Bertini, I. (1990). Identification of localized redox states in plant-type two-iron ferredoxins using the nuclear Overhauser effect, *Biochemistry* **29**, 2263–2271.

Dunham, W. R., Palmer, G., Sands, R. H., and Bearden, A. J. (1971). On the structure of the iron-sulfur complex in the two-iron ferredoxins, *Biochim. Biophys. Acta* **253**, 373–384.

Evans, D. J., and Leigh, G. J. (1991). The coordination of esters of amino acids to $\{Fe_4S_4\}^{2+}$ clusters, *J. Inorg. Biochem.* **42**, 25–35.

Fukuyama, K., Hase, T., Matsumoto, S., Tsukihara, T., Katsube, Y., Tanaka, N., Kakudo, M., Wada. K., and Matsubara, H., (1980). Structure of *S. platensis* [2Fe–2S] ferredoxin and evolu-

tion of chloroplast-type ferredoxins, *Nature (London)* **286**, 522–524.

Gerber, N. C., Horiuchi, T., Koga, H., and Sligar, S. G. (1990). Identification of 2Fe-2S cysteine ligands in putidaredoxin, *Biochem. Biophys. Res. Commun.* **169**, 1016–1020.

Gomez-Moreno, C., Sancho, J., Fillat, M. F., Pueyo, J. J., and Edmondson, D. E. (1987). Complex formation between ferredoxin-$NADP^+$-oxidoreductase and flavodoxin, in *Flavins and Flavoproteins 1987* (Edmondson, D. E., and McCormick, D. B., eds.), deGruyter, Berlin, pp. 335–339.

Greenfield, N. J., Wu, X., and Jordan, F. (1989). Proton magnetic resonance spectra of adrenodoxin: features of the aromatic region, *Biochim. Biophys. Acta* **995**, 246–254.

Gurbiel, R. J., Batie, C. J., Sivaraja, M., True, A. E., Fee, J. A., Hoffman, B. M., and Ballou, D. P. (1989). Electron-nuclear double resonance spectroscopy of ^{15}N-enriched phthalate dioxygenase from *Pseudomonas cepacia* proves that two histidines are coordinated to the [2Fe-2S] Rieske-type clusters, *Biochemistry* **28**, 4861–4871.

Gurbiel, R. J., Ohnishi, T., Robertson, D. E., Daldal, F., and Hoffman, B. M. (1991). Q-Band ENDOR spectra of the Rieske protein from *Rhodobactor capsulatus* ubiquinol-cytochrome *c* oxidoreductase show two histidines coordinated to the [2Fe-2S] cluster. *Biochemistry* **30**, 11579–11584.

Hazzard, J. T., McLendon, G., Cusanovich, M. A., Das, G., Sherman, F., and Tollin, G. (1988). Effects of amino acid replacements in yeast iso-1 cytochrome *c* on heme accessibility and intracomplex electron transfer in complexes with cytochrome *c* peroxidase. *Biochemistry* **27**, 4445-4451.

Hazzard, J. T., Rong, S. Y. and Tollin, G. (1991). Ionic strength dependence of electron transfer from bovine mitochondrial cytochrome *c* to bovine cytochrome *c* oxidase, *Biochemistry* **30**, 213–222.

Hervas, M., Navarro, J. A. and Tollin, G. (1992). A laser flash spectroscopy study of the kinetics of electron transfer from spinach Photosystem I to spinach and algal ferredoxins. *Photochem. Photobiol.* **56**, 319–324.

Houseman, A. L. P., Oh, B.-H., Kennedy, M C., Fan, C., Werst, M. M., Beinert, H., Markley, J. L., and Hoffman, B. M. (1992). $^{14,15}N$, ^{13}C, ^{57}Fe, $^{1,2}H$ Q-band ENDOR study of Fe-S proteins with clusters that have endogenous sulfur ligands, *Biochemistry* **31**, 2073–2080.

Hurley, J. K., Salamon, Z., Meyer, T. E., Fitch, J. C., Cusanovich, M. A., Markley, J. L., Cheng, H., Xia, B., Chae, Y. K., Medina, M., Gomez-Moreno, C., and Tollin, G. (1993a). Amino acid residues in *Anabaena* ferredoxin crucial to interaction with ferredoxin-$NADP^+$ reductase: site-directed mutagenesis and laser flash photolysis, *Biochemistry*, **32**, 9346–9354.

Hurley, J. K., Cheng, H., Xia, B., Markley, J. L., Medina, M., Gomez-Moreno C., and Tollin, G., (1993b). An aromatic amino acid residue is required at position 65 in *Anabaena* ferredoxin for rapid electron transfer to ferredoxin: $NADP^+$ reductase, *J. Am. Chem. Soc.*, in press.

Jacobson, B. L., Chae, Y. K., Böhme, H., Markley, J. L., and Holden, H. M. (1992). Crystallization and preliminary analysis of oxidized recombinant heterocyst [2Fe-2S] ferredoxin from *Anabaena* 7120, *Arch. Biochem. Biophys.* **294**, 279–281.

Jacobson, B. L., Chae, Y. K., Markley, J. L., Rayment, I., and Holden, H. M. (1993a). Molecular structure of the oxidized, recombinant, heterocyst [2Fe-2S] ferredoxin from *Anabaena* 7120 determined to 1.7 Å resolution, *Biochemistry* **32**, 6788–6793.

Jacobson, B. L., Cheng, H., Markley, J. L., and Holden, H. M. (1993b), in preparation.

Karplus, P. A., Daniels, M. J., and Herriott, J. R. (1991). Atomic structure of ferredoxin-$NADP^+$ reductase: prototype for a structurally novel flavoenzyme family, *Science* **251**, 60–66.

Kassner, R. J., and Yang, W. (1977). A theoretical model for the effects of solvent and protein dielectric on the redox potentials of iron–sulfur clusters, *J. Am. Chem. Soc.* **99**, 4351–4355.

Kraulis, P. J. (1991). MOLSCRIPT: a program to produce both detailed and schematic plots of protein structures, *J. Appl. Crystallogr.* **24**, 946–950.

Kunkel, T. A., Roberts, J. D., and Zakour, R. A. (1987). Rapid and efficient site-specific mutagenesis without phenotypic selection, *Methods Enzymol.* **154**, 367–382.

Masaki, R., Yoshikawa, S., and Matsubara, H. (1982). Steady-state kinetics of oxidation of reduced ferredoxin with ferredoxin-$NADP^+$ reductase, *Biochim. Biophys. Acta* **700**, 101–109.

Mason, J. I., and Boyd, G. S. (1971). The cholesterol side-chain cleavage enzyme system in mitochondria of human term placenta, *Eur. J. Biochem.* **21**, 308–321.

Matsubara, H., and Hase, T. (1983). Phylogenetic consideration of ferredoxin sequences in plants, particularly algae, in *Proteins and Nucleic Acids in Plant Systematics* (Jensen, U., and Fairbrothers, D. E., eds.), Springer-Verlag, Berlin, Heidelberg.

Matsubara, H., Hase, T., Wakabayashi, S., and Wada K. (1980). Structure and evolution of chloroplast- and bacterial-type ferredoxin, in *The Evolution of Protein Structure and Function* (Sigman, D. S., and Brazier, H. A. B., eds.), Academic Press, New York, pp. 245–266.

Mauro, J. M., Fishel, L. A., Hazzard, J. T., Meyer, T. E., Tollin, G., Cusanovich, M. A., and Kraut, J. (1988). Tryptophan-191 → phenylalanine, a proximal-side mutation in yeast cytochrome *c* peroxidase that strongly affects the kinetics of ferrocytochrome *c* oxidation, *Biochemistry* **27**, 6243–6256.

Meyer, T. E., Rivera, M., Walker, F. A., Mauk, M. R., Mauk, A. G., Cusanovich, M. A., and Tollin, G. (1993). Laser flash photolysis studies of electron transfer to the cytochrome b_5-cytochrome *c* complex, *Biochemistry* **32**, 622–627.

Mittal, S., Zhu, Y.-Z., and Vickery, L. E. (1988). Molecular cloning and sequence analysis of human placental ferredoxin, *Arch. Biochem. Biophys.* **264**, 383–391.

Miura, S., and Ichikawa, Y. (1991a). Proton nuclear magnetic resonance investigation of adrenodoxin. Assignment of aromatic resonances and evidence for a conformational similarity with ferredoxin from *Spirulina platensis*, *Eur. J. Biochem.* **197**, 747–757.

Miura, S., and Ichikawa, Y. (1991b). Conformational change of adrenodoxin induced by reduction of iron-sulfur cluster, *J. Biol. Chem.* **266**, 6252–6258.

Mooberry, E. S., Oh, B.-H., and Markley, J. L. (1989). Improvement of ^{13}C-^{15}N chemical shift correlation spectroscopy by implementing time proportional phase incrementation, *J. Magn. Reson.* **85**, 147–149 (1989).

Oh, B.-H., and Markley, J. L. (1990a). Multinuclear magnetic resonance studies of the 2Fe-2S* ferredoxin from *Anabaena* sp. strain PCC 7120: 1. Hydrogen-1 resonance assignments and secondary structure in solution of the oxidized form, *Biochemistry* **29**, 3993-4004.

Oh, B.-H., and Markley, J. L. (1990b). Multinuclear magnetic resonance studies of the 2Fe-2S* ferredoxin from *Anabaena* sp. strain PCC 7120: 3. Detection and characterization of hyperfine-shifted nitrogen-15 and hydrogen-1 resonances of the oxidized form, *Biochemistry* **29**, 4012-4017.

Oh, B.-H., Westler, W. M., Darba, P., and Markley, J. L. (1988). Protein carbon-13 spin systems by a single two-dimensional nuclear magnetic resonance experiment, *Science* **240**, 908–911.

Oh, B.-H., Westler, W. M., and Markley, J. L. (1989). Carbon-13 spin system directed strategy for assigning cross peaks in the COSY fingerprint region of a protein, *J. Am. Chem. Soc.* **111**, 3083–3085.

Oh, B.-H., Mooberry, E. S., and Markley, J. L. (1990). Multinuclear magnetic resonance studies of the 2Fe-2S* ferredoxin from

Anabaena sp. strain PCC 7120: 2. Sequence-specific carbon-13 and nitrogen-15 resonance assignments of the oxidized form, *Biochemistry* **29**, 4004-4011.

Okamura, T., John, M. E., Zuber, M. X., Simpson, E. R., and Waterman, M. R. (1985). Molecular cloning and amino acid sequence of the precursor form of bovine adrenodoxin: Evidence for a previously unidentified COOH-terminal peptide, *Proc. Natl. Acad. Sci. USA* **82**, 5705–5709.

Peterson, J. A., Lorence, M. C., and Amarneh, B. (1990). Putidaredoxin reductase and putidaredoxin. Cloning, sequence determination, and heterologous expression of the proteins, *J. Biol.* Chem. **265**, 6066–6073.

Pochapsky, T. C., and Ye, X. M. (1991). ^{1}H NMR identification of a β-sheet structure and description of folding topology in putidaredoxin, *Biochemistry* **30**, 3850–3856.

Poe, M., Phillips, W. D., Glickson, J. D., and San Pietro, A. (1971). Proton magnetic resonance studies of the ferredoxins from spinach and parsley. *Proc. Natl. Acad. Sci. USA* **68**, 68–71.

Przysiecki, C. T., Bhattacharyya, A. K., Tollin, G., and Cusanovich, M. A. (1985). Kinetics of reduction of *Clostridium pasteurianum* rubredoxin by laser photoreduced spinach ferredoxin : $NADP^+$ reductase and free flavins, *J. Biol. Chem.* **260**, 1452–1458.

Rayment, I., Wesenberg, G., Meyer, T. E., Cusanovich, M. A., and Holden, H. M. (1992). Three-dimensional structure of the high-potential iron-sulfur protein isolated from the purple phototrophic bacterium *Rhodocyclus tenuis* determined and refined at 1.5 Å resolution, *J. Mol. Biol.* **228**, 672–686.

Robbins, A. H., and Stout, C. D. (1989). Structure of activated aconitase: formation of the [4Fe-4S] cluster in the crystal, *Proc. Natl. Acad. Sci. USA* **86**, 3639–3643.

Rothery, R. A., and Weiner, J. H. (1991). Alteration of the iron-sulfur composition of *Escherichia coli* dimethyl sulfoxide reductase by site-directed mutagenesis, *Biochemistry* **30**, 8296–8305.

Rypniewski, W. R., Breiter, D. R., Benning, M. M., Wesenberg, G., Oh, B.-H., Markley, J. L., Rayment, I., and Holden, H. M. (1991). Crystallization and structure determination to 2.5 Å resolution of the oxidized [2Fe-2S] ferredoxin isolated from *Anabaena* 7120, *Biochemistry* **30**, 4126–4131.

Salamon, Z., and Tollin, G. (1992). Cyclic voltammetric behavior of [2Fe-2S] ferredoxins at a lipid bilayer modified electrode, *Bioelectrochem. Bioenerg.* **27**, 381–391.

Sambrook, J., Fritsch, E. F., and Maniatis, T. (1989). *Molecular Cloning, A Laboratory Manual*, Cold Spring Harbor Laboratory Press, Plainview, New York.

Sanger, F., Niklen, S., and Coulson, A. R. (1977). DNA sequencing with chain-terminating inhibitors, *Proc. Natl. Acad. Sci. USA* **74**, 5463–5467.

Schrautemeier, B., and Böhme, H. (1985). A distinct ferredoxin for nitrogen fixation isolated from heterocysts of the cyanobacterium *Anabaena variabilis*, *FEBS Lett.* **184**, 304–308.

Skjeldal, L., Westler, W. M., and Markley, J. L. (1990). Detection and characterization of hyperfine shifted resonances in the proton NMR spectrum of *Anabaena* 710 ferredoxin at high magnetic fields, *Arch. Biochem. Biophys.* **278**, 482–485.

Skjeldal, L., Markley, J. L., Coghlan, V. M., and Vickery, L. (1991a). Hydrogen-1 NMR spectra of vertebrate [2Fe-2S] ferredoxins. Hyperfine resonances suggest different electron delocalization patterns from plant ferredoxins, *Biochemistry* **30**, 9078–9083.

Skjeldal, L., Westler, W. M., Oh, B.-H., Krezel, A. M., Holden, H. M., Jacobson, B. L., Rayment, I., and Markley, J. L. (1991b). Two-dimensional magnetization exchange spectroscopy of *Anabaena* 7120 ferredoxin. Nuclear Overhauser effect and electron self-exchange cross peaks from amino acid residues surrounding the 2Fe-2S* cluster, *Biochemistry* **30**, 7363–7368.

Springer, B. A., and Sligar, S. G. (1987). High-level expression of sperm whale myoglobin in *Escherichia coli*, *Proc. Nat. Acad. Sci., USA* **84**, 8961–8965.

Stockman, B. J., and Markley, J. L. (1990). Stable-isotope assisted protein NMR spectroscopy in solution, in *Advances in Biophysical Chemistry*, Vol. 1 (Bush, C. A., ed.), JAI Press, Greenwich, Connecticut, pp. 1–46.

Sussman, J. L., Shoham, M., and Harel, M. (1989). Protein adaptation to extreme salinity: the crystal structure of 2Fe2S ferredoxin from *Halobacterium Marismortui*, in *Computer-Assisted Modeling of Receptor–Ligand Interactions: Theoretical Aspects and Applications to Drug Design*, Alan R. Liss, New York, pp. 171–187.

Ta, D. T., and Vickery, L. E. (1992). Cloning, sequencing, and overexpression of a [2Fe-2S] ferredoxin gene from *Escherichia coli*, *J. Biol. Chem.* **267**, 11120–11125.

Tanaka, M., Haniu, M., Yasunobu, K. T., Roa, K. K., and Hall, D. O. (1976). The complete amino acid sequence of *Spirulina platensis* ferredoxin, *Biochem. Biophys. Res. Commun.* **69**, 759–765.

Tollin, G., and Hazzard, J. T. (1991). Intra- and intermolecular electron transfer processes in redox proteins, *Arch. Biochem. Biophys.* **287**, 1–7.

Tollin, G., Hurley, J. K., Hazzard, J. T., and Meyer, T. E. (1993). Use of laser flash photolysis time-resolved spectrophotometry to investigate interprotein and intraprotein electron transfer mechanisms, *Biophys. Chem.*, in press.

Tsukihara, T., Fukuyama, K., Nakamura, M., Katsube, Y., Tanaka, N., Kakudo, M., Wada, K., Hase, T., and Matsubara, H. (1981). X-ray analysis of a [2Fe-2S] ferredoxin from *Spirulina platensis*. Main chain fold and location of side chains at 2.5 Å resolution, *J. Biochem.* **90**, 1763–1773.

Tsukihara, T., Fukuyama, K., and Katsube, Y. (1986). Structure–function relationship of [2Fe-2S] ferredoxins, in *Iron-Sulfur Protein Research* (Matsubara, H., Katsube, Y., and Wada, K., eds.), Japan Sci. Soc. Press, Tokyo, pp. 59–68.

Tsukihara, T., Fukuyama, K., Mizushima, M., Harioka, T., Kusunoki, M., Katsube, Y., Hase, T., and Matsubara, H. (1990). Structure of the [2Fe-2S] ferredoxin I from the blue-green alga *Aphanothece sacrum* at 2.2 Å resolution, *J. Mol. Biol.* **216**, 399–410.

Walker, M. C., Pueyo, J. J., Gomez-Moreno, C., and G. Tollin (1990). Comparison of the kinetics of reduction and intramolecular electron transfer in electrostatic and covalent complexes of ferredoxin-$NADP^+$ reductase and flavodoxin from *Anabaena* PCC 7119, *Arch. Biochem. Biophys.* **281**, 76–83.

Walker, M. C., Pueyo, J. J., Navarro, J. A., Gomez-Moreno, C., and Tollin, G. (1991). Comparison of the kinetics of reduction and intramolecular electron transfer in electrostatic and covalent complexes of ferredoxin-$NADP^+$ reductase and flavodoxin from *Anabaena* PCC 7119, *Arch. Biochem. Biophys.* **287**, 351–358.

Werth, M. T., Cecchini, G., Manodori, A., Acdrell, B. A. C., Schröder, I., Gunsalus, R. T., and Johnson, M. K. (1990). Site-directed mutagenesis of conserved cysteine residues in *Escherichia coli* fumarate reductase: modification of the spectroscopic and electrochemical properties of the [2Fe-2S] cluster, *Proc. Natl. Acad. Sci. USA* **87**, 8965–8969.

Wishart, D. S., Sykes, B. D., and Richards, F. M. (1992). The chemical shift index: a fast and simple method for the assignment of protein secondary structure through NMR spectroscopy, *Biochemistry* **31**, 1647–1651.

Xia, B., Cheng, H., Skjeldal, L., Coghlan, V. M., Vickery, L. E., and Markley, J. L. (1993). Multinuclear magnetic resonance and mutagenesis studies of the histidine residues of human placental ferredoxin, in preparation.

Ye, X. M., Pochapsky, T. C., and Pochapsky, S. S. (1992). ^{1}H NMR

sequential assignments and identification of secondary structural elements in oxidized putidaredoxin, and electron–transfer protein from *Pseudomonas*, *Biochemistry* **31**, 1961–1968.

Zanetti, G. and Merati, G. (1987). Interaction between photosystem I and ferredoxin. Identification by chemical cross-linking of the polypeptide which binds ferredoxin, *Eur. J. Biochem.* **169**, 143–146.

Zanetti, G., Morelli, D., Ronchi, S., Negri, A., Aliverti, A., and Curti, B. (1988). Structural studies on the interaction between ferredoxin and ferredoxin-$NADP^+$ reductase, *Biochemistry* **27**, 3753–3759.